Two Novel Related Yeast Nucleoporins Nup170p and Nup157p: Complementation with the Vertebrate Homologue Nup155p and Functional Interactions with the Yeast Nuclear Pore–Membrane Protein Pom152p

John D. Aitchison,* Michael P. Rout,* Marcello Marelli,‡ Günter Blobel,* and Richard W. Wozniak‡

*The Laboratory of Cell Biology, Howard Hughes Medical Institute, The Rockefeller University, New York 10021; and ‡Department of Anatomy and Cell Biology, University of Alberta, Edmonton, AB, Canada, T6G 2A7

Abstract. We have taken a combined genetic and biochemical approach to identify major constituents of the yeast nuclear pore complex (NPC). A synthetic lethal screen was used to identify proteins which interact genetically with the major pore–membrane protein Pom152p. In parallel, polypeptides present in similar amounts to Pom152p in a highly enriched preparation of yeast NPCs have been characterized by direct microsequencing. These approaches have led to the identification of two novel and major nucleoporins, Nup170p and Nup157p. Both Nup170p and Nup157p are similar to each other and to an abundant mammalian nucleoporin, Nup155p (Radu, A., G. Blobel, and R. W. Wozniak. 1993. *J. Cell Biol.* 121: 1–9) and interestingly, *nup170* mutants can be complemented with mammalian *NUP155*. In addition, the synthetic lethal screen identified genetic interactions between Pom152p and two other major nucleoporins, Nup188p (Nehrbass, U., S. Maguire, M. Rout, G. Blobel, and R. W. Wozniak, manuscript submitted for publication), and Nic96p (Grandi, P., V. Doye, and E. C. Hurt. 1993. *EMBO J.* 12: 3061–71). We have determined that together, Nup170p, Nup157p, Pom152p, Nup188p, and Nic96p comprise greater than one-fifth of the mass of the isolated yeast NPC. Examination of the genetic interactions between these proteins indicate that while deletion of either *POM152*, *NUP170*, or *NUP188* alone is not lethal, pairwise combinations are. Deletion of *NUP157* is also not lethal. However, *nup157* null mutants, while lethal in combination with *nup170* and *nup188* null alleles, are not synthetically lethal with *pom152* null alleles. We suggest that Nup170p and Nup157p may be part of a morphologically symmetrical but functionally distinct substructure of the yeast NPC, e.g., the nucleoplasmic and cytoplasmic rings. Finally, we observed morphological abnormalities in the nuclear envelope as a function of alterations in the expression levels of *NUP170* suggesting a specific stoichiometric relationship between NPC components is required for the maintenance of normal nuclear structure.

COMMUNICATION between the cytoplasm and the nucleoplasm is controlled by nuclear pore complexes (NPCs)[1] which extend across the nuclear envelope (NE) at circular openings along the surface of the nucleus. The NPCs are tightly associated with the NE via the pore membrane domain, a specialized subdomain of the NE which lines the pore and connects the outer and inner nuclear membranes. A major function of the NPC is to regulate the bidirectional transport of proteins and ribonucleoproteins between the cytoplasm and the nucleoplasm. The mechanism of macromolecular traffic is signal mediated, stepwise, energy dependent (reviewed in Forbes, 1992), and requires cytosolic factors (Newmeyer and Forbes, 1990; Adam et al., 1990; Moore and Blobel, 1992, 1993; Adam and Adam, 1994; Görlich et al., 1994; Morioanu et al., 1995; Radu et al., 1995*a*; Görlich et al., 1995; Mattaj, 1995; Enenkel et al., 1995). In addition to its role in transport, the ordered arrangement of NPCs along the nuclear surface (Maul, 1977) has been proposed to reflect a role for NPCs in the three-dimensional organization of the underlying chromatin (Blobel, 1985).

The detailed structure of the NPC has been determined at the highest resolution in vertebrates. Each NPC is an octagonally symmetric cylindrical structure. The core framework of the NPC, some 120 nm in diameter and 70 nm along its cylindrical axis, appears to be composed of sev-

Address correspondence to Richard W. Wozniak, Department of Anatomy and Cell Biology, 5-14 Medical Sciences Building, University of Alberta, Edmonton, Alberta, Canada, T6G 2A7. Ph.: 403-492-1384. Fax: 403-492-0450. e-mail: rwozniak@anat.med.ualberta.ca.

1. *Abbreviations used in this paper*: ORF, open reading frame; NE, nuclear envelope; NPC, nuclear pore complex; nups, nucleoporins; poms, pore membrane proteins; SM, synthetic minimal medium.

eral coaxial rings which are interconnected by struts and buttresses, surrounding a variably present central plug or transporter (Hinshaw et al., 1992; Akey and Radermacher, 1993). More peripheral structures such as the cytoplasmic particles, cytoplasmic filaments, and nuclear cages have been found projecting more than 50 nm from the nuclear and cytoplasmic faces of the core structure (Unwin and Milligan, 1982; Jarnik and Aebi, 1991; Goldberg et al., 1992; Ris and Melecki, 1993).

The recent isolation and more detailed structural analysis of the yeast NPC (Rout and Blobel, 1993) supports the long-held view that the overall structure and organization of the NPC is well conserved among all eukaryotes (Maul, 1977). The conserved ultrastructure of the NPC likely reflects conserved structural features present in its polypeptide constituents. This has, in part, been observed for a related family of nucleoporins (or nups, a general terminology used to refer to NPC proteins) that have been molecularly characterized in vertebrates and yeast, all of which contain repetitive peptide motifs (Nup1p, Nup2p, Nsp1p, Nup49p, Nup57p, Nup100p, Nup116p, Nup145p, Nup159p, from yeast and p62, Nup98p, Nup153p, Nup214p, and Nup358p from vertebrates; reviewed in Rout and Wente, 1994; Gorsch et al., 1995, Grandi et al., 1995; Kraemer et al., 1995; Wu et al., 1995). Four of the vertebrate nucleoporins from this family have been sublocalized by immunoelectron microscopy to peripheral structures of the pore. Nup214p (Kraemer et al., 1994) and Nup358p (Wu et al., 1995) are localized to the cytoplasmic filaments; Nup153p (Sukegawa and Blobel, 1993) and Nup98p (Radu et al., 1995*b*) are present in the nuclear cage. Although proteins of this family contain primary sequence similarities within the repeat regions, functional intra- or interspecies complementation has not been demonstrated.

Only a handful of other nucleoporins and integral pore–membrane proteins or POMs (designated as such for their sublocalization to this domain of the nuclear pore) have been molecularly characterized. These include the nucleoporins Nup155p, Nup107p, and Tpr (Byrd et al., 1995) (Nup266p) from vertebrates, Nic96p and Nup133p in yeast, and the POMs gp210 and Pom121p in vertebrates and Pom152p in yeast (reviewed in Rout and Wente, 1994). Yeast Pom152p and Nic96p and vertebrate gp210 and Nup155p are the most abundant of the nups and poms so far identified in their respective organisms and as such probably play a fundamental role in the subunit organization of the underlying NPC framework. With the exception of Pom121p which contains FXFG repeats and a 20–amino acid residue segment similar to Pom152p (Hallberg et al., 1993; Wozniak et al., 1994), the sequence of each of these polypeptides is unique and unrelated to one another. In light of the morphological conservation of the NPC, much insight into important conserved components of the NPC may be expected from the identification of functional homologues between divergent phyla. So far, however, no such homologues have been identified.

As a step towards characterizing the structure and function of the NPC framework, we have taken a combined genetic and biochemical approach. We have used a *POM152* synthetic lethal screen to identify proteins which interact with this major pore–membrane protein. In parallel, polypeptides present in similar amounts to Pom152p in a highly enriched preparation of yeast NPCs have been characterized by direct microsequencing. This has led to the identification of a major yeast nucleoporin, termed Nup170p, that interacts genetically with Pom152p and when depleted (in the absence of Pom152p) leads to abnormalities in the morphology of the nuclear envelope. In addition, another abundant nucleoporin, termed Nup157p, was identified in the NPC fraction which bears striking sequence similarity to Nup170p but is functionally distinct. These two nucleoporins are structurally similar to mammalian Nup155p which, when expressed in yeast, incorporates into the NPC and functionally complements *nup170* mutants.

Materials and Methods

Yeast Strains and Media

Relevant yeast strains used in this study are listed in Table I. All strains were grown as described (Sherman et al., 1986) in YPD (1% yeast extract, 2% bactopeptone, and 2% glucose), YPGal (1% yeast extract, 2% bactopeptone, and 2% galactose), or synthetic minimal media (SM) supplemented with the appropriate amino acids and 2% glucose. 5-FOA–containing plates were made as described (Ausubel et al., 1992). All strains were grown at 30°C unless otherwise stated. Procedures for yeast manipulation were conducted as described by Sherman et al. (1986). Transformation of yeast was performed by electroporation (Delorme, 1989).

Plasmids

The plasmids used in this study are as follows: pRS315, *CEN/LEU2* (Sikorski and Hieter, 1989); pRS316, *CEN/URA3* (Sikorski and Hieter, 1989); pRS424, *2μm/TRP1* (Christianson et al., 1992); pSB32 *CEN/LEU2*; pCH1122, *CEN/URA3/ADE3*; (Kranz and Holm, 1990; kindly provided by C. Holm, Harvard University, Boston, MA); pEMBLyex4, *2μm/Leu2d/URA3/CYC1-GAL10* (Cesareni and Murray, 1987; kindly provided by U. Nehrbass, Rockefeller University, New York); pPOM152, pRS315 containing a 6.8-kb BamHI/BamHI insert encoding the *POM152* open reading frame (ORF) plus its flanking promoter and terminator sequences; pCH1122-POM152, the complete *POM152* ORF and its promoter (contained in a 5.1-kb BamHI/BclI fragment from pPOM152) inserted into a BamHI site of pCH1122; p2105, pSB32 with a 9.2-kb genomic DNA insert containing the *NUP170* ORF; pHNP170, pRS315 carrying a 6.3-kb HpaI/HpaI fragment containing the *NUP170* ORF; p2105B, p2105 lacking a 2.1-kb BamHI fragment; pUN100-NIC96 (*CEN/LEU2*, Grandi et al., 1993; kindly provided by E. Hurt, EMBL, Heidelberg, Germany); p33, pSB32 containing the *NUP188* locus (Nehrbass, U., S. Maguire, M. Rout, G. Blobel, and R. W. Wozniak, manuscript submitted for publication); pNUP188U, pRS316 containing the *NUP188* locus (Nehrbass, U., S. Maguire, M. Rout, G. Blobel, and R. W. Wozniak, manuscript submitted for publication); pADH155; pRS424 containing the ADH1 promoter (a kind gift from E. Johnson, Rockefeller U., New York; Ammerer, 1983) inserted into the KpnI/SalI sites and a 4.5-kb *NUP155* cDNA SalI/BglII fragment from λgt11 (Radu et al., 1993) inserted into the SalI/BamHI sites. The plasmids used for gene disruptions are described below.

Isolation of POM152 Synthetic Lethal (psl) Mutants

A colony sectoring assay (Kranz and Holm, 1990; Bender and Pringle, 1991) was used to identify mutants in which *POM152* had become essential for viability. The haploid strain PM152-75 was transformed with the plasmid pCH1122-POM152. The resulting strain, PM152-CP, was UV mutagenized on YPD plates with a Stratalinker (Stratagene, La Jolla, CA) (14 mJ/cm^2) to a viability of ~15%. These plates were then incubated at 30°C for 5–8 d. Approximately 200,000 colonies were screened to identify red, nonsectoring (sec$^-$) mutants. After extended growth on YPD, 61 sec$^-$ strains were identified of which 34 were Ura$^+$ and failed to grow on media containing 5-FOA (5-FOA$_s$). The sec$^+$ phenotype and the ability to grow on 5-FOA (5-FOA$_r$) could be restored to 32 mutants by transformation with the plasmid pPOM152 (*CEN/LEU2*) but not with pRS315 alone.

Table I. Yeast Strain Genotype

Strain	Genotype	Derivation
W303	*Mata/Matα ade2-1/ade2-1 ura3-1/ura3-1 his3-11,15/his3-11,15 trp1-1/trp1-1 leu2-3,112/leu2-3,112 can1-100/can1-100*	
DF5	*Mata/Matα ura3-52/ura3-52 his3-Δ200/his3-Δ200 trp1-1/trp1-1 leu2-3,112/leu2-3,112 lys2-801/lys2-801*	
PMY17	*Mata ade2-1 ura3-1 his3-11,15 trp1-1 leu2-3,112 can1-100 pom152-2::HIS3*	Wozniak et al., 1994
CH1462	*Matα ade2 ade3 ura3 his3 leu2 can1*	Kranz and Holm, 1990
PM152CH	*Mata/Matα ade2/ade2 ade3/ADE3 ura3-1/ura3-1 his3/his3 trp1/TRP1 leu2/leu2 can1/can1 pom152-2::HIS3/+*	Cross of PMY17xCH1462
PM152-75	*Matα ade2 ade3 ura3 his3 trp1 leu2 can1 pom152-2::HIS3*	Segregant of sporulated PM152CH
PM152W	*Mata ade2 ade3 ura3 his3 TRP1 leu2 can1 pom152-2::HIS3*	Segregant of sporulated PM152CH
PM152-CP	*Matα ade2 ade3 ura3 his3 trp1 leu2 can1 pom152-2::HIS3 pCH1122-POM152(ADE3-URA3)*	Transformant of PM152-75 with pCH1122-POM152
psl21	*Matα ade2 ade3 ura3 his3 trp1 leu2 can1 pom152-2::HIS3 nup170-21 pCH1122-POM152(ADE3-URA3)*	Synthetic lethal from PM152CP
NP170Δ	*Mata/Matα ade2-1/ade2-1 ura3-1/ura3-1 his3-11,15/his3-11,15 trp1-1/trp1-1 leu2-3,112/leu2-3,112 can1-100/can1-100 nup170-1::HIS3/+*	Integrative transformation of W303 with 5′-NUP170-HIS3-NUP170-3′ fragment from pNup170-HIS
NP170-11.1	*Matα ade2-1 ura3-1 his3-11,15 trp1-1 leu2-3,112 can1-100 nup170-1::HIS3*	Segregant of sporulated NP170Δ
NP188-2.2	*Mata ade2-1 ura3-1 his3-1 his3-11,15 trp1-1 leu2-3,112 can1-100 nup188-1::HIS3*	See text
NP188-2.4	*Matα ade2-1 ura3-1 his3-1 his3-11,15 trp1-1 leu2-3,112 can1-100 nup188-1::HIS3*	See text
NP170/PM152	*Mata/Matα ade2-1/ade2-1 ura3-1/ura3-1 his3-11,15/his3-11,15 trp1-1/trp1-1 leu2-3,112/leu2-3,112 can1-100/can1-100 nup170-1::HIS3/+ pom152-2::HIS3/+ pCH1122-POM152 (ADE3-URA3)*	Cross of NP170-11.1 xPM152-W transformed with pCH1122-POM152
NP170/NP188	*Mata/Matα ade2-1/ade2-1 ura3-1/ura3-1 his3-11,15/his3-11,15 trp1-1/trp1-1 leu2-3,112/leu2-3,112 can1-100/can1-100 nup170-1::HIS3/+ nup188-1:HIS3/+* pNUP188U *(URA3)*	Cross of NP170-11.1 xNP188-2.2 transformed with pNUP188U
NP170/PM152-2A	*Mata ade2 ade3 ura3 his3 trp1 leu2 can1 nup170-1::HIS3 pom152-2::HIS3 pCH1122-POM152 (ADE3-URA3)*	Segregant of sporulated NP170/PM152 containing pCH1122-POM152
NP170/NP188-54	*Matα ade2-1 ura3-1 his3-11,15 trp1-1 leu2-3,112 can1-100 nup170-1::HIS3 nup188-1:HIS3 pNUP188U(URA3)*	Segregant of sporulated NP170/NP188 containing pNUP188U
NP157Δ	*Mata/Matα ura3-52/ura3-52 his3-Δ200/his3-Δ200 trp1-1/trp1-1 leu2-3,112/leu2-3,112 lys2-801/lys2-801 nup157-2::URA3/+*	Integrative transformation of DF5 with URA3 flanked by NUP157 linkers
NP157-2.1	*Mata ura3-52 his3-Δ200 trp1-1 leu2-3,112 lys2-801 nup157-2::URA3*	Segregant of sporulated NP157Δ
NP170/NP157	*Mata/Matα ade 2-1/ade2-1 ura3-1/ura3-1 his3-11,15/his3-11,15 trp1-1/trp1-1 leu2-3,112/leu2-3,112 can1-100/can1-100 nup170-1::HIS3/+ nup157-2::URA3/+*	Cross of NP170-11.1 xNP157-2.1
NP188/NP157	*Mata/Matα ade2-1/ade2-1 ura3-1/ura3-1 his3-11,15/his3-11,15 trp1-1/trp1-1 leu2-3,112/leu2-3,112 can1-100/can1-100 nup188-1::HIS3/+ nup157-2::URA3/+*	Cross of NP188-2.4 xNP157-2.1
PM152/NP157	*Mata/Matα ade2-1/ ade2-1 ura3-1/ura3-1 his3-11,15/his3-11,15 trp1-1/trp1-1 leu2-3,112/leu2-3,112 can1-100/can1-100 pom152-2::HIS3/+ nup157-2::URA3/+*	Cross of PM152-75 xNP157-2.1
NP170/PM152-155	*Matα ade2 ade3 ura3 his3 trp1 leu2 can1 nup170-1::HIS3 pom152-2::HIS3 pADH155-(TRP1)*	NP170/PM152-2A transformed with pADH155- and selected on 5-FOA
NP170UG	*Mata/Matα ade2-1/ade2-1 ura3-1/ura3-1 his3-11,15/his3-11,15 trp1-1/trp1-1 leu2-3,112/leu2-3,112 can1-100/can1-100 nup170-2::URA3-GAL10/+*	Integrative transformation of W303 with 5′-NUP170-URA3-GAL10-NUP170-3′ fragment from pNUP170UG
NP170UG-60.2	*Mata ade2-1 ura3-1 his3-11,15 trp1-1 leu2-3,112 can1-100 nup170-2::URA3-GAL10*	Segregant of sporulated NP170UG
NP170UG/PM152	*Mata/Matα ade2-1/ade2-1 ura3-1/ura3-1 his3-11,15/his3-11,15 trp1-1/trp1-1 leu2-3,112/leu2-3,112 can1-100/can1-10 nup170-2::URA3-GAL10/+ pom152-2::HIS3/+*	Cross of NP170UG-60.2xPM152-75
NP170UG/PM152-1	*Mata ade2-1 ura3-1 his3-11,15 trp1-1 leu2-3,112 can1-100 nup170-2::URA3-GAL10 pom152-2::HIS3*	Segregant of sporulated NP170UG/PM152
NP170pA	*Mata/Matα ura3-52/ura3-52 his3-Δ200/his3-Δ200 trp1-1/trp1-1 leu2-3,112/leu2-3,112 lys2-801/lys2-801 nup170-protA (URA3-HIS3)/+*	Integrative transformation of DF5 with ProteinA-*His3-Ura3* at the 3′ end of *NUP170*
NP157pA	*Mata/Matα ura3-52/ura3-52 his3-Δ200/his3-Δ200 trp1-1/trp1-1 leu2-3,112/leu2-3,112 lys2-801/lys2-801 nup157-protA (URA3-HIS3)/+*	Integrative transformation of DF5 with ProteinA-*His3-Ura3* at the 3′ end of *NUP157*

Backcrosses to the parent strain indicated that each of the mutations was recessive. The diploid derived from a cross with psl21 was sporulated and tetrads were dissected. The resulting haploids showed a 2:2 segregation of the mutant phenotype suggesting a single mutation was responsible for the sec$^-$ phenotype. This strain was initially chosen for complementation (see below). Similar analyses were also conducted in various other mutants where it was necessary to establish that a single locus was responsible for the sec$^-$ phenotype.

Complementation of the psl Mutants

To identify the wild-type allele for the *psl* mutant, psl21, the strain was transformed by electroporation with a yeast genomic DNA library inserted into pSB32 (*CEN/LEU2*) (kindly provided by J. Rine, University of California, Berkeley, CA). Transformants were plated on SM-leucine plates and grown for 5–8 d at 30°C. Three Sec$^+$ and 5-FOA$_r$ colonies were selected. Plasmids were isolated from each strain and propagated by shuttling into the *Escherichia coli* strain DH5α (Strathern and Higgins, 1991). Isolated plasmids were then reintroduced into psl21 to confirm their ability to rescue the sec$^-$ and 5-FOA$_s$ phenotypes. Restriction analysis revealed that two of the plasmids contained the same insert and the third contained a unique but overlapping insert. The plasmid containing the smallest insert (9.2 kb), p2105, was partially sequenced using Sequenase (United States Biochemical Corp., Cleveland, OH) and synthetic oligonucleotide primers corresponding to plasmid sequence flanking the insert. A comparison of this sequence with available databases revealed that the insert was derived from the left arm of *Saccharomyces cerevisiae* chromosome II. The complementing activity of the p2105 insert was narrowed to a 6.3-kb HpaI/HpaI fragment containing a single complete ORF previously designated YBL079w (Fig. 2; plasmid pHNP170).

To examine the ability of the YBL079w ORF to complement additional *psl* mutants, the p2105 plasmid was transformed into the remaining mutants. p2105 restored the sec$^+$/5-FOA$_r$ phenotype in five additional mutants. All six of the mutants are allelic to YBL079w (hereafter termed *NUP170*). Crosses of these mutants with the haploid strain NP170/PM152-2A (*pom152Δ nup170Δ*) produced diploids which failed to grow on 5-FOA.

Gene Disruptions

Deletion/disruption of the *NUP170* and the *NUP157* genes was performed by integrative transformation using the procedure of Rothstein (1991). The *NUP170* gene was disrupted using a DNA fragment assembled in Bluescript SK(−) (Stratagene, La Jolla, CA) which consisted of three separate DNA fragments arranged in the following order: (*a*) a fragment corresponding to a 580 bp region immediately 5′ to the *NUP170* initiation codon; (*b*) a BamHI/BamHI DNA fragment containing the *HIS3* selectable marker isolated from the plasmid pJJ217 (Jones and Prakash, 1990); and (*c*) an 817 bp fragment beginning with the codon for amino acid residue 1499 of the *NUP170* ORF and extending 817 bp 3′ of the *NUP170* ORF. Both the 5′ and 3′ regions flanking the *NUP170* gene were synthesized using the polymerase chain reaction (PCR) and appropriate sense and antisense primers. The resulting plasmid was termed pNUP170-His. The disruption fragment was used to transform the diploid strain W303 and His$^+$ transformants were selected on SM-histidine plates. His$^+$ strains were analyzed by Southern blotting to identify heterozygous diploids carrying the *nup170::HIS3* disrupted gene. Cells from the disrupted strain NP170Δ were sporulated and tetrads were dissected on YPD plates. All spores were viable and the *HIS3* marker segregated with the expected 2:2 ratio. The absence of the *NUP170* gene in the His$^+$ segregants was confirmed by Southern blotting.

The DNA fragment used for disruption of the *NUP157* gene was derived by PCR-directed amplification of the *URA3* gene using the following primers with overhangs corresponding to *NUP157*:

sense primer: 5′-GCT CGG ATT TCA ATT GTG ATG TAT TCA ACT CCA CTA AAA AAG AGG ATT GAT TAC GAT CGC CAG AGC AGA TTG TAC TGA GAG TGC-3′

antisense primer: 5′-CGT TCA TTT CAG GCC ATG ATG ACG ATC CTT CTC ATA ATC TTG AAC GGG ATC GGT ATT CGG ATC TGT GCG GTA TTT CAC ACC-3′

The 5′ region of the sense and antisense primers corresponds to nucleotides −18 to +42 and +4179 to +4117 of *NUP157* (where +1 = A of the initiation codon), respectively. The 3′ region of each primer corresponds to the sequence surrounding the insertion site of the *URA3* gene in pRS316. The PCR product was precipitated and transformed into DF5 cells by electroporation. Transformants were screened for the presence of the *URA3*-disrupted *NUP157* gene by the PCR using a primer within the *URA3* gene and a second primer in the 3′ untranslated region of *NUP157* and Southern blotting using standard techniques. Tetrads from the clone NP157Δ were dissected; all spores were viable, and the *URA3* marker segregated 2:2.

GAL10 Promoter Replacement of NUP170

The *GAL10* promoter, fused downstream of a *URA3* marker, was integrated into the genome immediately upstream of the *NUP170* initiation codon in wild-type (W303) cells as for the gene disruptions. The linear DNA fragment used for the transformation was synthesized using the PCR from a DNA fragment assembled in Bluescript SK(−) (Stratagene) consisting of three separate DNA fragments arranged in the following order: (*a*) an ~500-bp fragment immediately 5′ to the *NUP170* initiation codon; (*b*) an ~1.3-kb DNA fragment containing the *URA3* selectable marker fused upstream of the *GAL10* promoter and the *CYC1* minimal promoter from pEMBLyex4 (Cesareni and Murray, 1987); and (*c*) a 900-bp fragment beginning with the initiation codon of the *NUP170* ORF and extending 3′ to the codon for amino acid residue 300. Both of the fragments derived from *NUP170* gene were synthesized using the PCR and appropriate sense and antisense primers. Proper integration of the promoter-replacement was confirmed by Southern blotting of Ura$^+$ diploids. Diploids were sporulated and tetrads were dissected onto galactose-containing medium. Ura$^+$ haploids were then crossed with the *pom152Δ* strain (PM152-75), tetrads were dissected as above and Ura$^+$ His$^+$ segregants were selected.

Isolation of Double Null Strains

Double null mutants of combinations of *NUP170*, *NUP188*, and *POM152* were generated as follows: The *nup170Δ* (*Δ* is used to signify a null allele) haploid strain (NP170-11.1) was crossed with *pom152Δ* (PM152W) and *nup188Δ* (NP188-2.2; Nehrbass, U., S. Maguire, M. Rout, G. Blobel, and R. W. Wozniak, manuscript submitted for publication) haploid strains and diploids were selected by complementation of auxotrophic markers. To ensure the viability of the subsequent meiotic products carrying the double mutations, pCH1122-POM152 (for the *nup170Δ* × *pom152Δ*) or pNUP188U (for the *nup170Δ* × *nup188Δ*) was introduced into the diploid strain. The resulting strains, NP170/PM152 and NP170/NP188 were sporulated and tetrads were dissected. Resulting haploids were scored for growth on SM-Histidine-Uracil and 5-FOA. Those haploids which were His$^+$/Ura$^+$/5-FOA$_s$ were analyzed by Southern blotting to determine whether they carried disrupted copies of *pom152::HIS3* and *nup170::HIS3* or *nup170::HIS3* and *nup188::HIS3* and that they lacked the corresponding wild-type genes. This analysis revealed that each of the His$^+$/Ura$^+$/5-FOA$_s$ haploids carried the appropriate double null mutations. Growth on 5-FOA of both the *nup170Δ pom152Δ* (NP170/PM152-2A) and *nup170Δ nup188Δ* (NP170/NP188-54) strains could be rescued by the introduction of pPOM152 (*LEU2*) or p33 (*NUP188/LEU2*), respectively.

Double null mutants of *NUP157*, *NUP170*, *POM152*, and *NUP188* were produced as follows: NP157Δ-2.1 cells, which were confirmed to contain a disrupted copy of *NUP157*, were crossed with PM152-75, NP170-11.1, NP188-2.4 and in each case the resulting diploids were sporulated. Approximately 20 tetrads from each cross were dissected and segregants were scored for growth on YPD and for the presence of both the *URA3* and *HIS3* markers. Haploid segregants derived from the *pom152Δnup157Δ* diploid strain (PM152/NP157) were all viable and one-half of the His$^+$ segregants were His$^+$/Ura$^+$. The dissection of tetrads from *nup170Δnup157Δ* (NP170/NP157) and *nup188Δnup157Δ* (NP188/NP157) diploids revealed an approximate ratio of 3:1 of viable:nonviable segregants. Of the viable haploids, one-third were His$^+$, one-third were Ura$^+$, and one-third Ura$^-$His$^-$. No His$^+$Ura$^+$ segregants were recovered.

Protein A Tagging of Nup170p and Nup157p

Genomic copies of the *NUP170* and *NUP157* genes were tagged by a COOH-terminal, in-frame integration of a DNA fragment encoding the IgG binding domains of protein A. The protein A gene and adjacent *HIS3* and *URA3* markers were amplified by the PCR from the plasmid pProtA/HU assembled in Bluescript SK(−) (Stratagene) in the following order: a 700-bp fragment encoding protein A inserted into the XbaI/EcoRI sites followed by the 1.2-kb *HIS3* gene in the EcoRI site and an XbaI/SphI

fragment of the *URA3* gene cloned into the XbaI/XhoI sites. The following primers were used for the PCR:

NUP170 sense primer: 5′-GAT CCA ATT GAA AAG TAC GTT AAG AAC AGC GGC AAT AAT TTG GGG ATT TGT TTC TAC AAA GAA GGT GAA GCT CAA AAA CTT AAT-3′

NUP170 antisense primer: 5′-ACC TTT ATC TTA AGG AAA AGT TCA CTC GAT ATT CTT AAC TTT ACC GTC TAG TAA GGC CTC TTT ACT TAT AAT ACA GTT TTT TAG-3′

NUP157 sense primer: 5′-GAT CCG AAT ACC GAT CCC GTT CAA GAT TAT GTG AAG GAT CGT CAT CAT GGC CTG AAA GGT GAA GCT CAA AAA CTT AAT-3′

NUP157 antisense primer: 5′-CCG TAA AAC AGC AGT TTA CAT TCA CTA TAT AAA GGA TGA CGT AAG AAT TTG CCT ACG TTT ACT TAT AAT ACA GTT TTT TAG-3′

The 5′ region of each sense primer encodes the carboxy terminus of either *NUP170* or *NUP157* (up to, but not including, the stop codon) and continues to encode the 21 nucleotides of protein A beginning at the glycine at amino acid residue 24 (Uhlen et al., 1984). The 5′ regions of the *NUP170* and *NUP157* antisense primers correspond to nucleotides +4629 to +4570 and +4282 to +4227 (where +1 is the A of the initiation codon), respectively, in the 3′ untranslated regions of *NUP170* and *NUP157* and continue to encode 24 nucleotides corresponding to the reverse complement of the *URA3* gene (nucleotides 1050–1027; Rose et al., 1984). The PCR products were transformed into DF5 cells by electroporation to insert an in frame, COOH-terminal fusion to the ORF of each gene producing either *NUP170-protein A* or *NUP157-protein A* followed by *HIS3* and *URA3*. His^+, Ura^+ colonies were replica plated onto nitrocellulose. The colonies were grown overnight on nitrocellulose and probed directly for protein A expression as follows: the filter was overlayed onto 1 M sorbitol, 20 mM EDTA, 50 mM dithiothreitol, and incubated at 37°C for 10 min, removed and overlayed onto 1 M sorbitol, 20 mM EDTA, 1 mg/ml zymolyase 100T, and then incubated for 3 h at 37°C. Spheroplasts were then lysed by transferring the filter onto Western transfer buffer (3 × 5 min; Burnette, 1981; Aitchison et al., 1991), followed by two washes by immersion of the filter in Tris-saline. The filters were then stained with amido black and probed by Western blotting as previously described (Burnette, 1981; Aitchison et al., 1991) using mouse anti–rabbit IgG followed by donkey anti–rabbit horseradish peroxidase and enhanced chemiluminescence (Amersham, Arlington Heights, IL). Of the 20 colonies screened, two positives were selected for each fusion and visualized by immunofluorescence microscopy.

Yeast Nuclear Pore Complex Protein Fractionation

The proteins comprising a highly enriched yeast nuclear pore complex fraction were separated by ion-exchange or SDS-hydroxylapatite chromatography followed by reverse–phase HPLC and SDS-PAGE as described (Rout and Blobel, 1993, Wozniak et al., 1994). Five abundant proteins with apparent SDS-PAGE mobilities ranging from ~150– ~170 kD and a polypeptide of ~90 kD were selected for further study; appropriate column fractions containing each of the proteins targeted for sequencing were individually pooled, separated by SDS-PAGE and transferred electrophoretically to polyvinyldiene difluoride membrane. After staining the membrane with 0.1% amido black in 10% acetic acid, bands corresponding to the individual proteins of interest were identified, excised, cleaved with endopeptidase Lys-C (Fernandez et al., 1994) and peptides subjected to NH_2-terminal sequence analysis.

The quantitation of the Coomassie-stained polypeptides was performed using a Pharmacia laser scanning densitometer (Pharmacia, Piscataway, NJ).

Microscopy

Immunofluorescence microscopy was done essentially as previously described (Kilmartin and Adams, 1984; Wente et al., 1992). Protein A chimeras were visualized in the NP170pA and NP157pA strains using mouse anti–rabbit IgG (preabsorbed against formaldehyde fixed wild-type yeast cells) followed by Cy-3–conjugated donkey anti–rabbit IgG (Jackson ImmunoResearch Laboratories, West Grove, PA).

Electron microscopy was done as previously described (Byers and Goetsch, 1991; Wente et al., 1992). For induction and repression of *NUP170* under control of the GAL promoter, NP170UG/PM152 cells were grown to mid-logarithmic phase in YP-raffinose (1% yeast extract, 2% bactopeptone, and 2% raffinose), washed with water and transferred to either YPD to repress or YP-gal to induce the expression of *NUP170* for the indicated length of time.

Results

Genetic Approaches to the Identification of Pom152p-interacting Proteins

The isolation and characterization of the yeast *POM152* gene (Wozniak et al., 1994) provided a unique opportunity to explore the interaction between a pore–membrane protein and associated structures of the NPC. Our previous observation that *pom152* null mutants are viable suggested that Pom152p may be a member of a family of functionally (though not necessarily structurally) related proteins whose other members, most likely nucleoporins (nups) or pore–membrane proteins (poms), compensate for its loss. To identify members of this putative family as well as those proteins which physically interact with Pom152p, we have isolated mutants in which *POM152* has become essential for cell viability. Mutants were identified using a red/white colony sectoring assay (Koshland et al., 1985) similar in design to those previously described (Krantz and Holm, 1990; Bender and Pringle, 1991) and used to identify proteins which interact with the yeast nucleoporins Nsp1p (Wimmer et al., 1992) and Nup1p (Belanger et al., 1994). The assay uses the color difference between *ade2* strains (red), and *ade2 ade3* strains (white). Transforming *ade2 ade3* strains with an autonomously replicating plasmid carrying the *ADE3* gene produces red colonies due to the presence of the wild-type *ADE3* gene product, with white sectors which arise from the spontaneous loss of the plasmid under nonselective conditions. If the cells are dependent on a gene product from the plasmid, the colonies remain uniformly red.

To screen for mutants dependent on plasmid-linked *POM152*, a *pom152Δ* strain (PM152-75) was transformed with the plasmid pCH1122-POM152 (containing the *URA3* and *ADE3* genes). When grown on nonselective medium, the resulting strain (PM152CP) exhibited a red/white sectoring phenotype (sec^+). Following UV mutagenesis, 34 nonsectoring mutants (sec^-) mutants were isolated which were dependent on the pCH1122-POM152 plasmid and sensitive to the addition of 5-FOA (5-FOA_s), a substrate toxic to cells with a functional *URA3* gene. The sec^+ and 5-FOA resistance (5-FOA_r) phenotype could be restored to 32 mutants by pPOM152(*LEU2*) indicating that these mutants were dependent on the *POM152* gene.

All 32 of the *POM152* synthetic lethal (*psl*) mutants isolated were recessive. Analysis of the haploid progeny from a cross of the parent strain with one of the *psl* mutants, psl21, revealed a 2:2 segregation pattern of the mutant suggesting a mutation in a single locus. To identify the corresponding wild-type allele, psl21 cells were transformed with a library of *S. cerevisiae* genomic DNA in the vector pSB32, a centromere-based plasmid containing the *LEU2* marker gene. Three clones were recovered which were sec^+ and 5-FOA_r. Plasmids recovered from these cells contained either of two overlapping inserts, the smallest of which (in plasmid p2105) was 9.2 kb in length. Of the *psl* mutants, p2105 rescued the Sec^+/5-FOA_r phenotype of

A

POM152 synthetic lethal strain (*psl*)	Transformed with LEU2-plasmid				
	pPOM152	p2105	pNIC96	p40	pNUP188
psl21	sec$^+$	sec$^+$	-	-	-
psl31	sec$^+$	sec$^+$	-	-	-
psl49	sec$^+$	sec$^+$	-	-	-
psl53	sec$^+$	sec$^+$	-	-	-
psl73	sec$^+$	sec$^+$	-	-	-
psl78	sec$^+$	sec$^+$	-	-	-
psl7	sec$^+$	-	sec$^+$	-	-
psl60	sec$^+$	-	sec$^+$	-	-
psl40	sec$^+$	-	-	sec$^+$	-
psl79	sec$^+$	-	-	sec$^+$	-
psl93	sec$^+$	-	-	sec$^+$	-

B

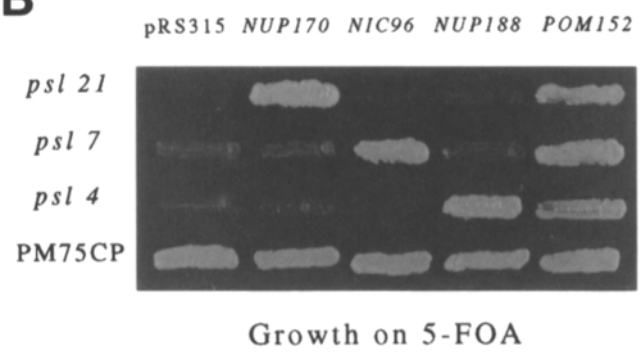

Figure 1. (*A*) Complementation of the *POM152* synthetic lethal (*psl*) mutants. The *psl* mutants examined can be grouped into four separate complementation groups. 11 mutants are shown in *A* which represent three groups. The sec$^-$ phenotype of each of these mutants can be rescued by a *CEN/LEU2* plasmid containing *POM152* (pPOM152). Six mutants are rescued by the plasmid p2105, two by pUN100-NIC96 (pNIC96), and three by the plasmid p40. pNUP188 fails to complement any of these mutants, but instead rescues a fourth complementation group composed of 20 *psl* mutants which are characterized elsewhere (Nehrbass, U., S. Maguire, M. P. Rout, G. Blobel, and R. W. Wozniak, manuscript submitted for publication). (*B*) Growth of rescued *psl* mutants on 5-FOA plates. Three representative mutants, psl21, psl7, psl4, and the parent strain PM75CP were grown on 5-FOA plates for 3 d at 30°C. All three mutants (containing the control plasmid pRS315) are 5-FOA$_s$ due to their requirement for the pCH1122-POM152 (*ADE3/URA3*) plasmid while PM75CP is 5-FOA$_r$. 5-FOA$_r$ can be restored to each mutant by the *POM152* gene in pRS315 (*CEN/LEU2*) (pPOM152; *POM152*). The 5-FOA$_r$ phenotype can also be restored to psl21 by the p2105 plasmid (*NUP170*), to psl7 by pUN100-NIC96 (*NIC96*; kindly provided by Ed Hurt, EMBL, Heidelberg, Germany), and to psl4 by a *NUP188*-containing plasmid p33 (*NUP188*; Nehrbass, U., S. Maguire, M. P. Rout, G. Blobel and R. W. Wozniak, manuscript submitted for publication).

five additional mutants (31, 49, 53, 73, and 78) suggesting they are members of a single complementation group (Fig. 1). Two additional complementation groups were similarly defined. One group, composed of twenty members, was complemented by the gene encoding a novel nucleoporin, Nup188p, and is characterized elsewhere (Nehrbass, U., S. Maguire, M. P. Rout, G. Blobel and R. W. Wozniak, manuscript submitted for publication). Members of the second group of four mutants were complemented by an uncharacterized plasmid termed p40 (Marelli, M. and R. W. Wozniak, unpublished results). Finally, two *psl* mutants were rescued by the plasmid pUN100-NIC96 (Fig. 1) containing the gene for a previously identified nucleoporin, Nic96p (Grandi et al., 1993).

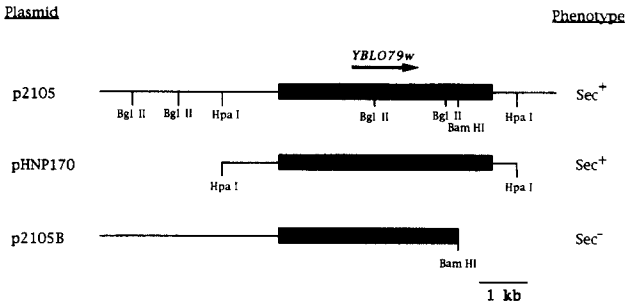

Figure 2. Map of the p2105 insert. The plasmid p2105 restores the sec$^+$/5-FOA$_r$ phenotype to six *psl* mutants (21, 31, 49, 53, 73, and 78). The p2105 insert corresponds to a 9.2-kb segment of *S. cerevisiae* chromosome II and contains a 4.5-kb ORF termed YBL079w. The position of relevant restriction sites within the insert are shown. The complementing activity of the p2105 insert has been narrowed to a 6.3-kb HpaI/HpaI fragment (pHNP170). A truncation with BamHI which removes the last 720 nucleotides of the YBL079w ORF (p2105B) abolishes its complementing activity.

Complementation of psl21 Identifies a Novel Yeast Nucleoporin, Nup170p, Which Is Similar to Both the Mammalian Nucleoporin Nup155p and an Uncharacterized Yeast Nucleoporin, Nup157p

We established by DNA sequence analysis that the p2150 insert corresponds to a 9.2-kb fragment of *S. cerevisiae* chromosome II. This fragment contains a 1,502–amino acid residue ORF designated YBL079w (accession no. sp P38181) with a deduced molecular mass of 170 kD (Fig. 2). Deletion analysis revealed that this gene alone can rescue the *psl* mutants complemented by p2105 (Fig. 2). Interestingly, a truncation of the p2105 which removed the last 240 amino-acid residues of the YBL079w ORF abolished its complementing activity (p2105B, Fig. 2). Finally, we have established that each of the mutants rescued by p2105 is allelic to the YBL079w locus (see Materials and Methods).

We have compared the sequence of the YBL079w ORF with available protein sequence data bases. The results of this search revealed that the YBL079w ORF shares significant sequence similarity (21.3% identity and 53.7% similarity) with the mammalian nucleoporin Nup155p (Radu et al., 1993; Fig. 3). In addition to Nup155p, searches of the data base with YBL079w also detected a closely related (41.7% identity and 78.4% similarity), uncharacterized ORF on the right arm of *S. cerevisiae* chromosome V (Fig. 3). This putative polypeptide, termed Yer105p (accession no. sp P40064), has a deduced molecular mass of 157 kD. The difference in the calculated molecular masses derived from the two ORFs is largely due to short insertions interspersed within the central third of the larger (YBL079w) ORF. On the basis of sequence similarities and both biochemical and in situ subcellular localization (see below),

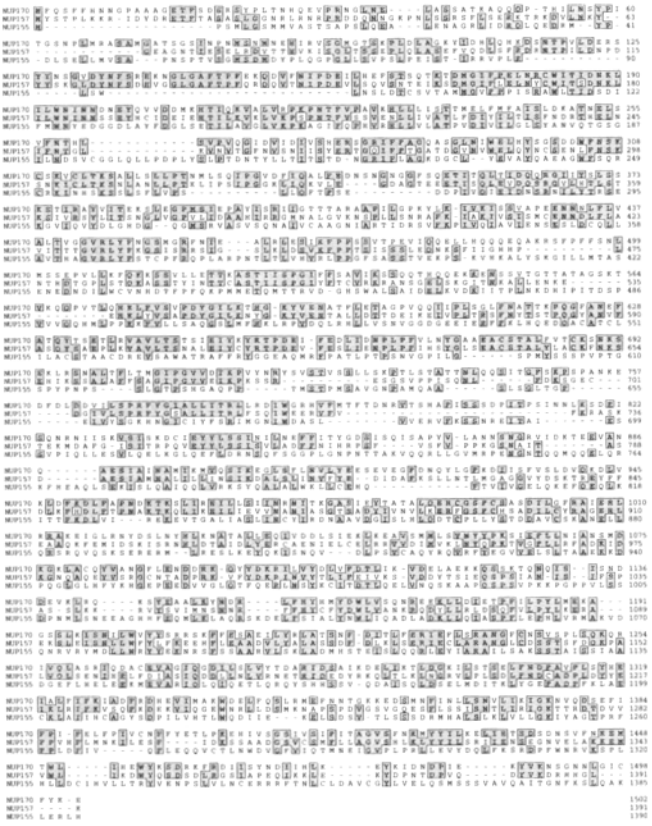

Figure 3. Alignment of the two yeast nucleoporins NUP170p and NUP157p, and the mammalian nucleoporin NUP155p. The triple alignment was done by the CLUSTAL method (Higgins and Sharp, 1989) using MegAlign software from DNASTAR (for multiple alignments: gap penalty = 10; gap length penalty = 10; for pairwise alignments: Ktuple = 1, gap penalty = 3, window = 5, diagonals saved = 5). Pairwise comparisons of each protein by the FASTA program (Pearson and Lipman, 1988) yielded the following results: NUP170p vs. NUP157p, 41.7% identity, 78.4% similarity; NUP170p vs. NUP155p, 21.3% identity, 53.7% similarity; NUP157p vs. NUP155p, 21.7% identity, 51.5% similarity (as calculated using the matrix file BLOSUM50 and gap penalties of −12/−2.) Identical amino acid residues (single letter code) are boxed and shaded.

we have renamed YBL079w and YER105c, *NUP170* and *NUP157*, respectively (following conventional nucleoporin nomenclature).

While Nup157p is more similar in mass to Nup155p, sequence comparisons suggest Nup155p is more closely related to Nup170p (Fig. 3). Further comparative analysis revealed certain highly conserved features present in Nup170p, Nup157p, and Nup155p. All three sequences contain an identical stretch of six amino acids residues, GVRLYF (residues 443–448 of Nup170p). In addition, each of the ten tryptophan residues in Nup170p is conserved in either Nup157p (9 of 10) or Nup155p (7 of 10) or both (6 of 10) suggesting they play an important functional role. As has been previously noted for Nup155p (Radu et al., 1993), both Nup170p and Nup157p contain an abundance of potential phosphorylation sites. The significance of these sites also remains to be determined. Kyte and Doolittle (1982) analysis of the hydropathic character of both Nup170p and Nup157p revealed no regions of significant hydrophobicity (and lacking charged residues) which could act as transmembrane segments. Finally, no sequence similarity was observed between Nup170p or Nup157p and Pom152p or any of the gene products which rescue other psl complementation groups including Nup188p and Nic96p.

Immunofluorescent Localization of Nup170p and Nup157p to the NPC

To examine the subcellular localization of Nup170p and Nup157p, both proteins were tagged with IgG binding domain of *Staphylococcal* protein A. This was accomplished by integrating the coding region of protein A into chromosomal copies of *NUP170* and *NUP157* following the last codon of their ORFs. The resulting strains were then examined by indirect immunofluorescence. Both Nup170–protein A and Nup157–protein A were visible along the surface of the nucleus in a punctate pattern characteristic of NPC localization (Fig. 4).

Nup170p and Nup157p Are Major Constituents of the Yeast NPC

A procedure has been previously described for the preparation of a highly enriched fraction of yeast NPCs (Rout and Blobel, 1993). The major feature of these isolated NPCs is the eightfold symmetry of their framework. When analyzed by SDS-PAGE, the NPC fraction revealed three prominent high molecular mass bands of 170, 160, and 150 kD that coenrich absolutely with the NPCs (cf. Fig. 3 *A*, *arrowheads*, Rout and Blobel, 1993). These can be further resolved on a 5–20% polyacrylamide gel into five distinct species: an intense, closely comigrating doublet at 170 kD, a less intense band at 160 kD, a strong band at 150 kD, and another less intense band just below that (Fig. 5). The identity of the 150-kD band had already been established (and reconfirmed here) as Pom152p (Wozniak et al., 1994; Fig. 5 *A*). To identify the other polypeptides, they were further purified (see Materials and Methods section) and each was analyzed by peptide microsequencing (Fig. 5 *B*). The lower band of the doublet at 170 kD is Nup188p (Nehrbass, U., S. Maguire, M. P. Rout, G. Blobel and R. W. Wozniak, manuscript submitted for publication) and the upper is an as yet uncharacterized protein. Microsequence derived from the 160-kD band yielded several peptides which identified it as Nup170p (Fig. 5, *A* and *B*). Similarly peptide sequence data from the band beneath Pom152p demonstrated that this polypeptide is Nup157p (Fig. 5 *B*).

Multiple chromatography procedures including SDS-hydroxylapatite chromatography, reverse-phase HPLC and ion-exchange chromatography suggest that Pom152p, Nup170p, Nup157p, Nup188p, and the upper 170 kD band are the only polypeptides within this molecular mass range in the NPC fraction (Wozniak et al., 1994; Rout and Blobel, 1993; data not shown). Moreover, all of the peptide sequences obtained from this region could be assigned to one of the above four proteins, with the exception of those obtained from the upper 170 kD species (data not shown). This allowed the relative amounts of all five Coomassie-blue stained polypeptides to be quantified by laser densi-

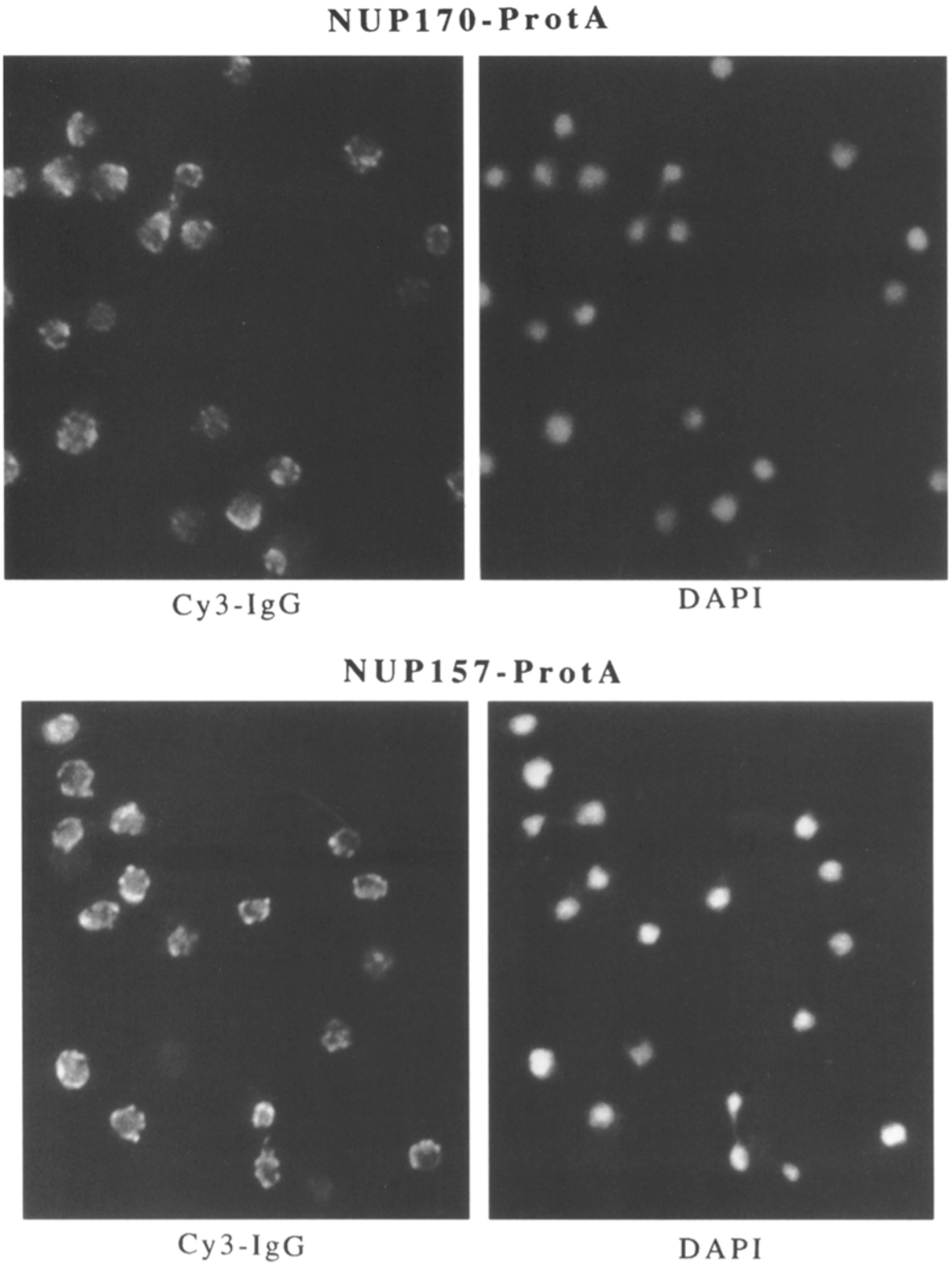

Figure 4. Immunofluorescence localization of NUP170p and NUP157p. The yeast strains NP170pA and NP157pA expressing the protein A–tagged *NUP170* and *NUP157* gene products, respectively, were formaldehyde-fixed, permeabilized, and probed with purified rabbit IgG followed by Cy3-labeled donkey anti–rabbit IgG (NUP170-protA and NUP157-protA). The nuclear DNA was visualized by coincident staining with DAPI. In each case the fusion proteins are visible along the nuclear surface in a punctate pattern characteristic of NPC localization. Bar, 5 μm.

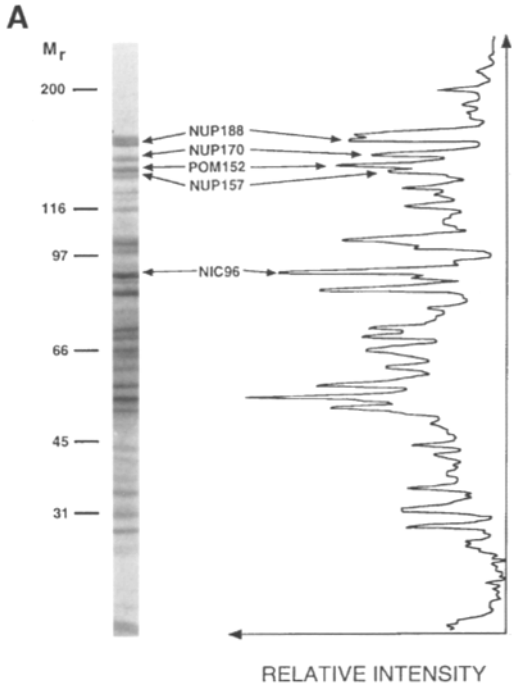

B

PEPTIDE SEQUENCE

Nup170p
117-NTPVLDERSYYNSGVDY-133
153-VFNIPDEILHEFST-166

Nup157p
1016-DDYTSIEQSPSIANI-1030
1349-DWYQSDSDLRGSIAPEQIK-1367

Nup188p
1187-ITDASLNLQYVNYEISTAK-1205
1611-YLNSRIIPTTLEEQQQLED-1629

Nic96p
276-YLEQQFLQYTDNLYK-290
103-IESEELEFYIRTK-115

Figure 5. NUP170p and NUP157p are major constituents of the yeast NPC. Polypeptides of the highly enriched NPC fraction were analyzed by SDS-PAGE (5–20% polyacrylamide gels) and visualized by Coomassie blue staining (*A*). Relative amounts of the proteins in this fraction were determined by a laser densitometry scan (*A*, *right*). Both the scan and gel are reproduced at the same scale and aligned with respect to each other. Arrows point to the positions of those particularly intense bands that have been determined to contain only a single protein, as shown by SDS-hydroxylapatite chromatography, reverse-phase HPLC and ion-exchange chromatography. The stated identity of each polypeptide was established by further purification and microsequence analysis of proteolytic fragments. Sequences derived from each of these polypeptides is shown in *B* in single letter code. The numbers flanking the peptide sequences correspond to the position of the first and last amino-acid residues in the cDNA-deduced sequence of the indicated polypeptide.

tometry. In combination with the calculated enrichment of the NPC fraction (Rout and Blobel, 1993), we estimated their relative contribution to the overall mass of the isolated NPCs (Fig. 5A). Each appeared to account for between 2 and 3 MD of the 66 MD measured for isolated yeast NPCs (Rout and Blobel, 1993). The yeast nucleoporin Nic96p (identified by microsequencing) is also similarly abundant (Fig. 5). Thus together, these six proteins could comprise as much as one-quarter of the mass of the isolated NPCs.

Deletion Mutants of nup170 and nup157 Are Viable

A deletion/disruption of the *NUP170* gene was performed to examine the phenotype of the *nup170* null mutant. The entire *NUP170* ORF was replaced with a DNA fragment encoding the *HIS3* gene by integrative transformation into the diploid strain W303. A His^+ transformant containing a disruption of *NUP170* (NP170Δ) was selected, sporulated, and tetrads were dissected. All four segregants from each tetrad were viable and exhibited a 2:2 segregation of the *HIS3* marker. His^+ haploids lacking the *NUP170* gene reproducibly formed smaller colonies when initially grown from individual spores (Fig. 6 *A*). However, after extended growth the *nup170Δ* strains divided at a rate similar to that observed in the presence of wild-type copy of *NUP170* at temperatures ranging from 17°–37°C (data not shown). Similarly, the entire ORF of *NUP157* was deleted and replaced with the *URA3* marker by integrative transformation into the diploid strain DF5. A diploid Ura^+ transformant with disruptions of the *NUP157* gene (*NP157Δ*) was selected and tetrads were dissected. All four segregants from each tetrad were viable (Fig. 6 *A*) and all tetrads showed a 2:2 segregation of the *URA3* marker. There was no detectable growth defect associated with the *nup157Δ* haploids. Thus both *nup170Δ* and *nup157Δ* exhibit a nonlethal phenotype similar to that observed for *pom152Δ* (Wozniak et al., 1994) and *nup188Δ* haploid strains (Nehrbass, U., S. Maguire, M. P. Rout, G. Blobel, and R. W. Wozniak, manuscript submitted for publication).

Genetic Interactions of NUP170, NUP157, POM152, and NUP188

Our battery of *psl* mutants indicated that both Nup170p and Nup188p interact genetically with Pom152p. In addition, the abundance of Nup157p and its similarity to Nup170p suggest that it may also interact genetically with this group of proteins. To further study the functional interactions between these four genes, double null mutants of each pair were constructed and their viability assayed by their dependence on a plasmid-born copy of one of the two genes. Initially *nup170Δ* (NP170-11.1) was crossed with *pom152Δ* (PM152-W) and *nup188Δ* (NP188-2.2) strains. Both of the resulting diploid strains carrying a *URA3* complementing plasmid (containing either *POM152* or *NUP188*) were sporulated and their haploid segregants assayed for growth on 5-FOA–containing plates (Fig. 6 *B*). None of the strains carrying the double deletions survived on 5-FOA. This growth defect, however, could be overcome by transformation with pPOM152 (*LEU2*) or p33 (*NUP188/LEU2*) (Fig. 6 *B*). Similar analysis also demonstrated a synthetic lethal phenotype associated with a *pom152Δ nup188Δ* double null strain (Nehrbass, U., S. Maguire, M. P. Rout, G. Blobel, and R. W. Wozniak, manuscript submitted for publication). Thus all combinations of double null mutants involving *nup170Δ*, *pom152Δ*, and *nup188Δ* are synthetically lethal, indicating a triad of genetic interactions.

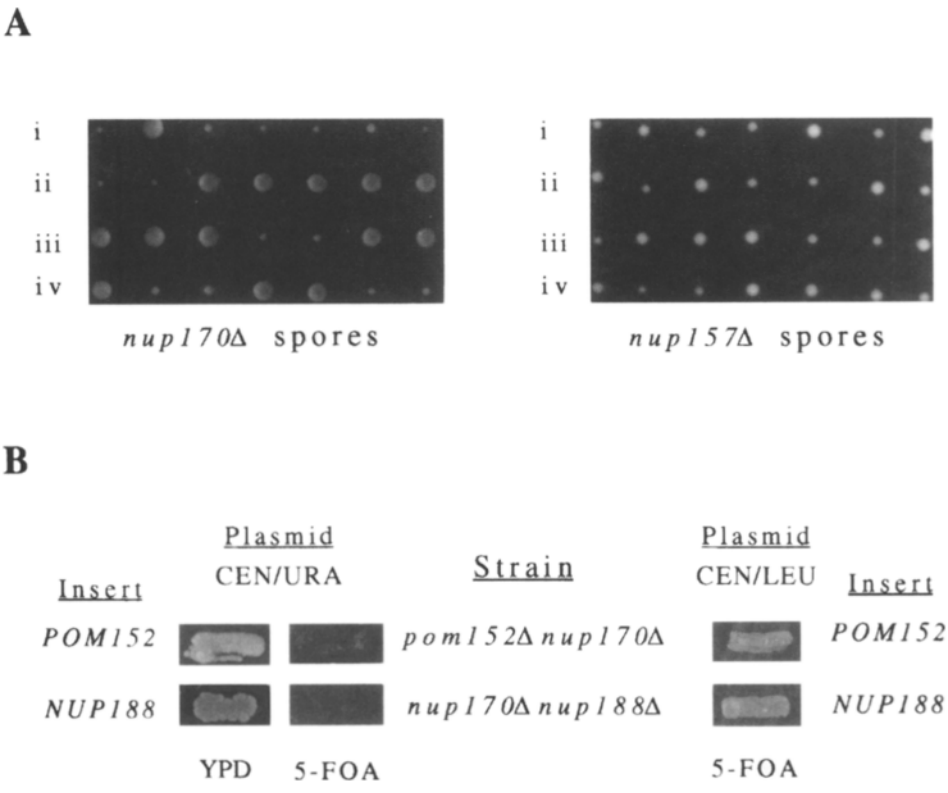

Figure 6. Analysis of *nup170* and *nup157* null mutations. (*A*) *nup170* and *nup157* null mutants are viable. Deletion and disruption of the *NUP170* gene was accomplished by replacement of the *NUP170* ORF with the *HIS3* selectable marker in the diploid strain W303. The *NUP157* gene was similarly disrupted by replacement of the *NUP157* ORF with the *URA3* selectable marker. In each case heterozygous diploids containing a wild-type and a disrupted copy of the *NUP* genes were sporulated and tetrads dissected on YPD plates. The haploid segregants following ~2 d of growth at 30°C are shown. While all four spores are viable in each case, a 2:2 segregation of large to small colonies was observed for *NUP170* disruption with the small colonies containing the disruption (His^+; data not shown). (*B*) Double disruptions of *pom152* and *nup170* and *nup170* and *nup188* are lethal. Two haploid strains, *pom152Δnup170Δ* and *nup170Δnup188Δ*, were isolated which contain a plasmid (*CEN/URA3*)-born copy of *POM152* and *NUP188*, respectively. Both strains were streaked on YPD and 5-FOA–containing plates and grown for 3 d at 30°C. Both strains are viable on YPD plates but fail to grow on 5-FOA plates. Introduction of *POM152* into *pom152Δnup170Δ* and *NUP188* into *nup170Δnup188Δ* on a separate *CEN/LEU2* plasmid complements the 5-FOA_s phenotype (*5-FOA*) under identical growth conditions.

To determine if a deletion of *NUP157* (*nup157-2::URA3*) is synthetically lethal in combination with deletions of either *NUP170* (*nup170-1::HIS3*), *NUP188* (*nup188-1::HIS3*) or *POM152* (*pom152-2::HIS3*), the appropriate crosses were made and Ura^+, His^+ diploids were selected. Diploids were sporulated and tetrads dissected. Analysis of haploid strains derived from *pom152Δnup157Δ* diploids (PM152/NP157) demonstrated that the *URA3* and *HIS3* markers segregated as unlinked non-interacting genes, indicating that there is no synthetic lethality resulting from the deletion of *NUP157* in combination with a deletion of *POM152* (data not shown). However, similar analysis of haploid segregants derived from *nup170Δnup157Δ* (NP170/NP157) and *nup188Δnup157Δ* (NP188/NP157) revealed a 3:1 segregation of viable:nonviable haploids. Of the viable haploids none were Ura^+, His^+ suggesting synthetic lethality (data not shown). Thus, while structurally similar, Nup157p and Nup170p appear functionally distinct.

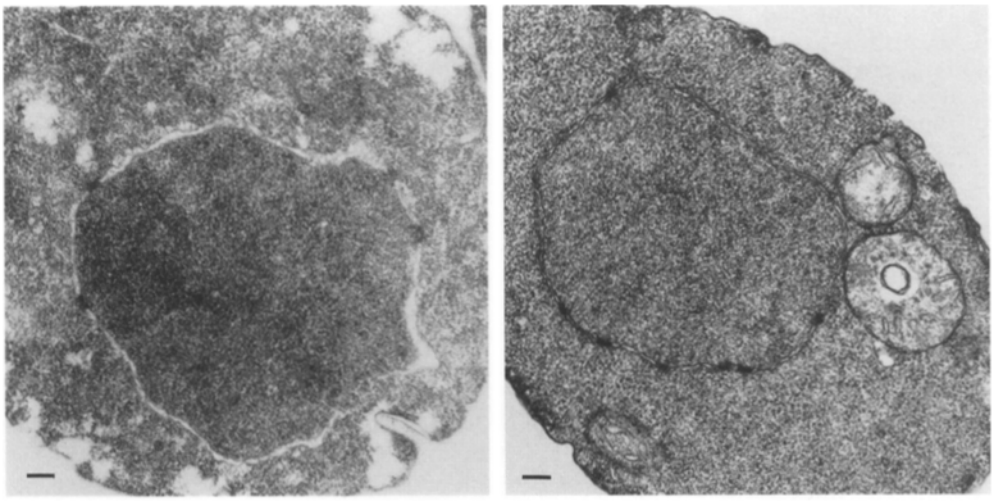

Figure 7. Thin-section electron micrographs of *pom152Δ* and *nup170Δ* cells. Cells (PMY17 and NP170-11.1) were grown in YPD at 30°C, fixed, and processed for electron microscopy. In both strains the morphology of the nucleus and nuclear envelope appear indistinguishable from wild-type cells. Bar, 0.2 μm.

Morphological Abnormalities Associated with Depletion and Overexpression of Nup170p

Given the lethal phenotype of *nup170Δ pom152Δ* strains, we investigated the morphological consequences of depletion and overexpression of the *NUP170* gene product in *POM152*-deleted cells. As a prerequisite for this study, we first examined the morphological phenotype of the null mutants *nup170Δ* (NP170-11.1) and *pom152Δ* (PMY17) strains by thin-section electron microscopy. In both cases these mutant cells showed no obvious structural abnormalities and appeared indistinguishable from wild-type cells (Fig. 7).

To vary the levels of Nup170p, its gene was placed under control of the *GAL10* promoter fused to the *CYC1* minimal promoter. The *GAL10* promoter, fused downstream of a *URA3* marker, was integrated into the genome immediately upstream of the *NUP170* initiation codon in wild-type (W303) and *pom152Δ* cells. Cells were then grown on either galactose to induce, or glucose to repress, expression of *NUP170*.

Cells carrying *NUP170* under the control of the *GAL10* promoter and a wild-type version of *POM152* (NP170UG-60.2) grew at rates similar to wild-type cells on either carbon source. Thin-section electron microscopy revealed no major apparent morphological abnormalities in these strains (Figs. 8 *A* and 9 *A*). In contrast, growth of *GAL10::nup170,pom152Δ* cells (the strain NP170UG/PM152-1) on glucose led to a moderate growth defect and dramatic alterations to their cellular morphology. These cells grew ~50% slower than *GAL10::nup170* cells containing wild-type *POM152* (data not shown). Light microscopy indicated that under these conditions the *GAL10::nup170,pom152Δ* cells were considerably larger than wild-type cells and usually contained large vacuoles (data not shown). Closer examination by electron microscopy revealed that the nuclear envelope in these cells had lost its regular shape and had developed massive extensions and invaginations (Fig. 8, *B–D*). Some of these invaginations appeared to surround cytoplasmic material including single-membrane bound vesicles (Fig. 8, *B* and *D*). The most likely interpretation of these images is that they represent cross-sectional views of large invaginations of the nuclear envelope which extend into the interior of the nucleus. While we see apparently normal NPCs, there are long stretches of nuclear envelope without detectable NPCs (Fig. 8 *B*). Areas this large devoid of NPCs could not be detected in wild-type cells and may reflect an overall reduction in the number of NPCs. In many cells there is a propensity of electron-dense material below the surface of the nuclear envelope (Fig. 8, *C* and *D*). These patches often lie juxtaposed to two double membranes.

It was surprising that although the *nup170Δ pom152Δ* double deletion is lethal, that *GAL10::nup170,pom152Δ* cells continued to grow on glucose for at least 36 h. Northern blot analysis indicated that although the expression of the *NUP170* mRNA was greatly induced when cells were grown on galactose, transfer to glucose did not completely repress the expression of the gene (data not shown). These results suggest that the nuclear envelope distortions observed in cells grown on glucose were the result of a decrease in the expression of *NUP170* and not the result of cell death. Consistent with these results, *GAL10::nup170, pom152Δ* cells, transformed with pCH1122-POM152 (*ADE3/POM152*) failed to sector on glucose over 10 d but sectored as efficiently as wild-type cells when grown on galactose (data not shown).

In contrast to the results observed with repressed *NUP170* expression, a distinct morphological phenotype was observed upon overexpression of *NUP170*. As was the case in glucose, *GAL10::nup170* cells (containing wild-type *POM152* NP170UG-60.2) grown on galactose to induce overexpression of *NUP170* showed no alterations in the structure of the nucleus or nuclear envelope (Fig. 9 *A*) as compared with wild-type strains. While appearing as wild-type in terms of the size and shape of the nucleus and nuclear envelope, galactose-induced overexpression of *NUP170* in *GAL10::nup170, pom152Δ* cells caused the appearance of structures resembling intranuclear annulate lamellae which lie parallel to and beneath the inner nuclear membrane (Fig. 9, *B–D*). As has been observed with cytoplasmic annulate lamellae in higher eukaryotes (Maul, 1977), NPCs within the intranuclear lamellae often appear in register with the NPCs present in the nuclear envelope with interconnecting, densely staining material (Fig. 9, *C* and *D*).

Mammalian Nup155p Can Functionally Replace Yeast Nup170p

We determined whether the similarities between Nup170p and mammalian Nup155p were sufficient to allow functional complementation of *nup170* mutants. A high-copy number plasmid, pADH155, containing *NUP155* under the control of the constitutive ADH promoter was introduced into the *nup170Δ pom152Δ* (NP170/PM152-1CH) and the psl21 strains, both of which are dependent on the plasmid pCH1122-POM152 and are thus 5-FOA$_s$. Several Trp$^+$ transformants were selected from each strain and then transferred to 5-FOA–containing plates. In each case 5-FOA$_r$ colonies appeared within 2 days (Fig. 10 *A*). No colonies were present in either untransformed cells (Fig. 10 *A*), cells transformed with the pRS424 alone, or in *nup188Δ pom152Δ* cells (data not shown). This demonstrated that the presence of Nup155p compensated for the loss of functional Nup170p in the synthetic lethal strains *pom152Δ nup170Δ* and psl21. It is of note that while *NUP155* complements the *nup170* mutants, the rescued strains grow at a slower rate than the corresponding strains rescued with *NUP170* (data not shown). Consistent with this observation, psl21 cells transformed with *NUP155* (pADH155) did not regain the ability to sector. These results suggest that the Nup155p-containing hybrid yeast NPCs fail to function with the same efficiency as wild-type yeast NPCs.

We examined the subcellular localization of Nup155p in *pom152Δnup170Δ* cells complemented with *NUP155* (NP170/PM152-155) by indirect immunofluorescence using antibodies directed against mammalian Nup155p (Radu et al., 1993). A survey of a field of cells revealed variations in the intensity of staining between individual cells, which likely reflects variations in the level of *NUP155* expression. At high levels of expression there was a great deal of speckled cytoplasmic staining as well as staining at the nu-

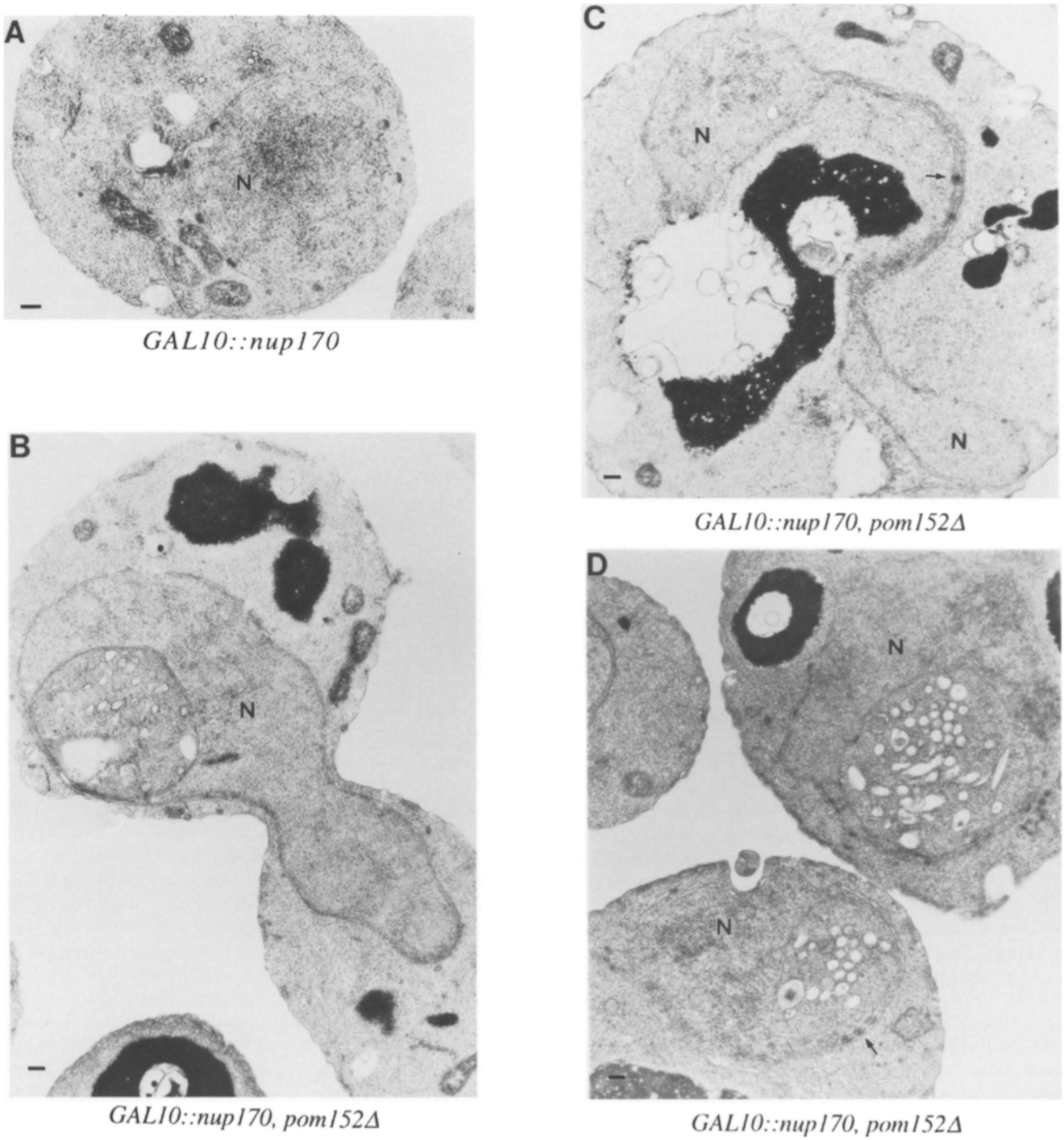

Figure 8. Depletion of NUP170p. Thin-section electron micrographs of cells expressing *NUP170* under the control of the *GAL10* promoter were grown on glucose to repress NUP170p synthesis in a wild-type background (*A*, NP170UG-60.2) or in a *pom152Δ* background (*B–D*, NP170UG/PM152-1). Cells were either maintained in YPD (*A*) or grown in YPD for 16 h (*B–D*) after transfer from 2% raffinose. The micrographs (*B–D*) depict large nuclear envelope invaginations and an overall loss of nuclear structure in the *GAL10::nup170, pom152Δ* cells. Arrows point to electron dense material below the surface of the nuclear envelope (*C* and *D*). These patches often lie juxtaposed to two double membranes. Bar, 0.2 μm.

clear periphery. At lower levels of expression Nup155p was concentrated at the nuclear periphery (Fig. 10 *B*), consistent with its localization to the NPC and its role in complementing the *nup170* mutants.

Discussion

We have identified a two-member family of structurally related, but functionally distinct, nucleoporins, Nup170p and Nup157p. Both Nup170p and Nup157p show a high

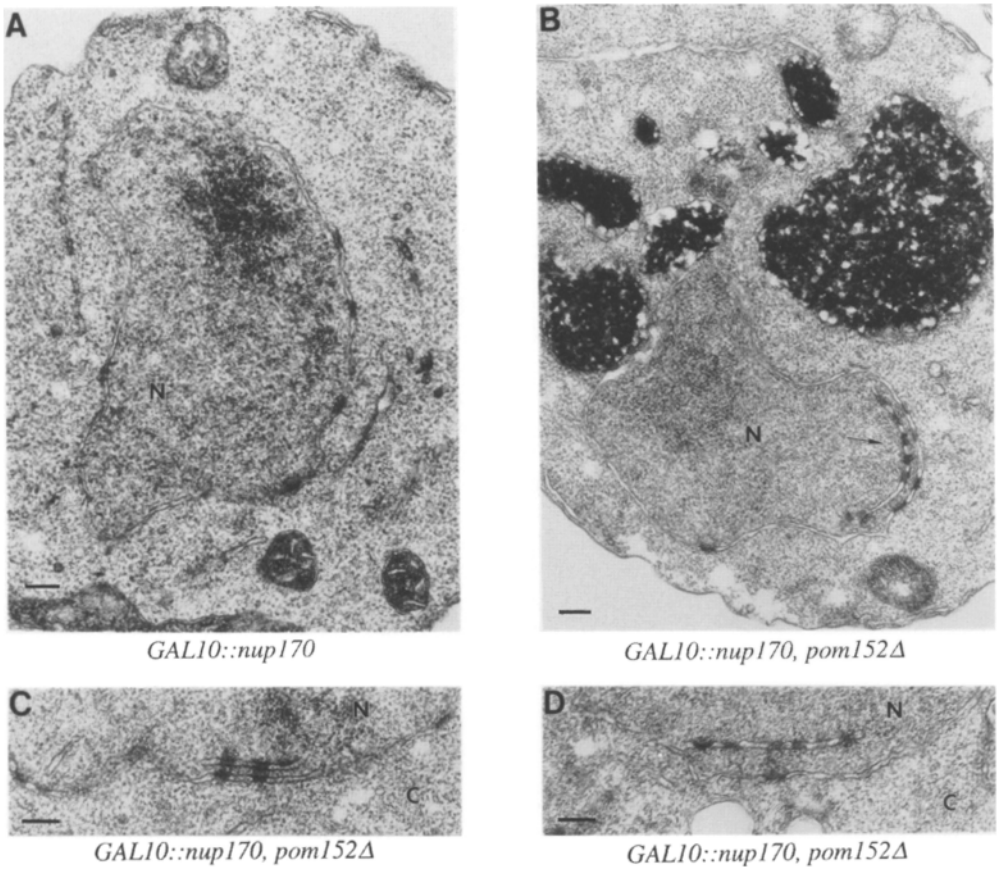

Figure 9. Overexpression of *NUP170*. Thin-section electron micrographs of cells expressing *NUP170* under the control of the *GAL10* promoter grown on 2% galactose to induce *NUP170* expression in a wild-type background (*A*, NP170UG-60.2) or in a *pom152Δ* background (*B-D*, NP170UG/PM152-1) are shown. Cells were either maintained in YP-gal (*A*) or grown in YP-gal for 16 h (*B-D*) after transfer from 2% raffinose. In contrast to depletion of Nup170p, galactose induced overexpression of *NUP170* in cells lacking *POM152* did not affect the gross structure of the nuclear envelope, however in many cases, intranuclear annulate lamellae were detected (*B-D*, *arrows*). Bar, 0.2 μm.

degree of sequence similarity with the mammalian nucleoporin Nup155p (Radu et al., 1993). This sequence similarity reflects an evolutionarily conserved role in NPC function as demonstrated by the ability of mammalian *NUP155* to functionally complement yeast mutants allelic to *NUP170*. We propose, on the basis of their sequence conservation, abundance, and interaction with other major NPC components, that these proteins play a fundamental role in the organization of the NPC framework.

Pom152p is an abundant integral membrane protein of the yeast NPC (Wozniak et al., 1994). With domains extending from the pore face (175 amino acids residues) and the lumenal face (1,141–amino acids residues) of the pore membrane, it is strategically located to play a role in the structural organization of the NPC and its anchorage to the pore membrane. Surprisingly, deletion of *POM152* is not lethal and it can be removed from the NPC without any apparent functional consequences. This suggests that design features built into the structure of the NPC allow it to maintain a minimal framework despite the loss of a major component. Thus, we sought out methods which might allow us to identify proteins which together with Pom152p contribute to the basic framework of the NPC structure.

Two approaches were taken. In the first, a genetic screen was designed based on synthetic lethality with *POM152*. Mutants identified by this screen presumably require either direct physical interactions with Pom152p or an overlapping function performed by Pom152p. We postulated that the wild-type alleles of these mutants would compensate for the loss of Pom152p in *pom152Δ* strains and, therefore, they would be expected to play an important structural role in the NPC. In the second approach we searched a highly enriched NPC fraction for proteins of similar abundance to Pom152p. This approach was based, in part, on the hypothesis that the framework of the NPC is composed of abundant and evolutionarily conserved proteins.

From the genetic screen, genes encoding three nucleoporins were identified which complement three *psl* complementation groups: Nup170p, which is characterized here, Nup188p, which is described in detail elsewhere (Nehrbass, U., S. Maguire, M. P. Rout, G. Blobel, and R. W. Wozniak, manuscript submitted for publication), and a previously identified nucleoporin, Nic96p (Grandi et al., 1993). In addition to their genetic interactions with Pom152p complementary biochemical approaches also established that all three of these proteins are major constituents of a highly enriched fraction of yeast NPCs. Microsequence analysis of another major protein in the NPC fraction initiated the characterization of the nucleoporin Nup157p which shows a high degree of sequence similarity to Nup170p. We estimate that Nup170p, Nup157p, Pom152p, Nup188p, and Nic96p are present in approximately 10–20 copies per NPC and together represent as much as 25% of the mass of the isolated yeast NPCs (Fig. 5).

Nup170p and Nup157p are both structurally similar to the mammalian nucleoporin, Nup155p (Fig. 3). Like its yeast counterparts, Nup155p is an abundant NPC protein and immunoelectron microscopy studies suggest that

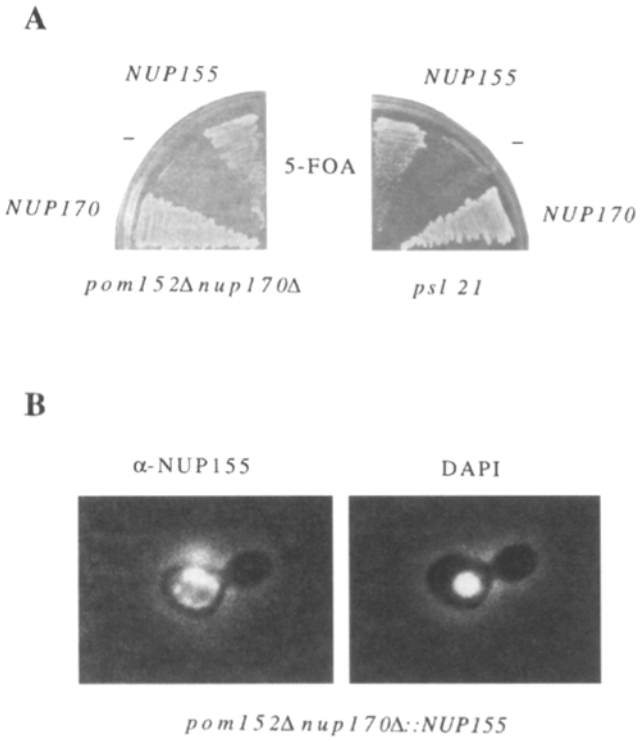

Figure 10. (*A*) Complementation of *nup170* mutations with mammalian *NUP155*. A cDNA encoding the rat nucleoporin Nup155p was inserted into the plasmid pRS424 (*TRP1*) downstream of the constitutive yeast ADH promoter. The resulting plasmid pADH155, and the p2105 plasmid containing *NUP170* were each transformed into two mutants allelic to *NUP170*; psl21 and the double null strain *pom152Δnup170Δ* (NP170/PM152-2A). Transformants were selected on SM-leu and then streaked on 5-FOA–containing plates and grown for 2 d at 30°C. Both untransformed psl21 and *pom152Δnup170Δ* (−) strains fail to grow on 5-FOA due to their requirement for the pCH1122-POM152 (*ADE3/URA3*) plasmid. p2105 complements the 5-FOAs phenotype of both mutants (*NUP170*). Strikingly, growth on 5-FOA is also restored to both mutants by pADH155 (*NUP155*) demonstrating that mammalian Nup155p can functionally replace yeast Nup170p. (*B*) Immunofluorescence localization of mammalian NUP155p to the nuclear periphery. The double-deletion mutant *pom152Δnup170Δ* harboring the plasmid pADH155 (NP170/PM152-155; labeled here *nup170Δ pom152Δ::NUP155*) was grown in YPD and processed for immunofluorescence. NUP155p was detected using rabbit anti–Nup155p peptide serum followed by mouse anti–rabbit Cy3 conjugate. The α-NUP155 shows the localization of NUP155p to the nuclear periphery using a combination of phase contrast and fluorescence microscopy. Coincident DAPI staining is shown (*right*).

Nup155p may be a component of the NPC core structure (Radu et al., 1993). By complementation of *nup170* mutants we have demonstrated that Nup155p can functionally replace Nup170p. This is the first example of such functional homology between yeast and vertebrate NPC proteins. The relationship between Nup155p and Nup157p, however, is unclear and awaits the isolation of the appropriate *nup157* mutants. In addition to the observed similarities between this set of proteins, searches of the database have also revealed a human cDNA with a deduced amino acid sequence highly similar (25.8% identity, 60.1% similarity; FASTA; Pearson and Lipman, 1988) to another major yeast nucleoporin, Nic96p. We have, in fact, established by microsequence analysis that a major polypeptide of ~90 kD in a fraction enriched in rat NPC proteins shows identity with the ORF of the human cDNA (Wozniak, R. W., and G. Blobel, unpublished data). The high degree of similarity between the yeast Nic96p and its mammalian counterpart suggests they too are homologues, but functional complementation remains to be examined.

Given the abundance of the Nup170p, Nup157p, Pom152p, Nup188p, and Nic96p it is remarkable that, with the exception of *NIC96* (Grandi et al., 1993), null mutants of each are viable. If, as we propose, these proteins are part of the major core structures of the NPC, the dispensability of each protein implies that the core framework is stabilized by multiple overlapping interactions. Thus under normal conditions, the scaffold can withstand the removal of any one of its struts or buttresses; but, if the structure is compromised by an additional loss, it is destabilized to the point of collapse. The presence of such multiple interactions is also suggested by the fact that we found *NIC96* in our genetic screen. The mutant form of Nic96p must be stabilized, at least in part, by the presence of Pom152p. Moreover, with the exception of Nup170p and Nup157p, these proteins lack any apparent sequence similarity, arguing against their role in a single redundant function.

Double disruptions of *POM152*, *NUP170*, and *NUP188*, in any combination, are lethal (Fig. 6 *B*). These data further support the results of the *POM152* synthetic lethal screen and suggest that Nup170p, Nup188p, and Pom152p all functionally interact. However, any direct physical interactions can only be inferred on the basis of their association with isolated NPCs. Conversely, while Nup157p is similarly abundant and structurally related to Nup170p, *nup157* null mutants, unlike those of *nup170*, are not synthetically lethal in combination with null mutants of *pom152*. These results suggest that Nup157p is functionally different from Nup170p and, possibly, part of a physically distinct substructure of the NPC which is unaffected by removal of Pom152p. This raises the intriguing possibility that Nup157p and Nup170p are structurally similar proteins in morphologically symmetrical, but physically and functionally distinct substructures of the NPC, such as the nuclear and cytoplasmic rings. Such similar proteins may provide the necessary asymmetry required for anchoring structures such as the cytoplasmic filaments and the nucleoplasmic cage.

In light of the functional conservation of Nup170p, we examined the effects of its depletion and overexpression. Varying the expression levels of *NUP170* produced no observable morphological changes in a wild-type background (Figs. 8 and 9). However, either repression or overexpression of *NUP170* in a *pom152* null background led to two separate and distinct phenotypes. First, depletion of Nup170p caused the development of enlarged and grossly distorted nuclear envelope membranes. This aspect of the phenotype is similar to the effects observed in *nup1* mutants (Bogerd et al., 1994). However, contrary to that reported for the *nup1* mutants, close examination of these cells revealed a distinct paucity of pores over large extended regions of the nuclear envelope (Fig. 8). In addition, structures resembling NPCs could be detected below

the double membrane, often between areas where invaginations placed two double membranes adjacent to one another. These structures may represent partially assembled NPCs which result from the depletion of Nup170p in the absence of Pom152p. They, however, do not appear to transport substrate as they do not form herniations of the type observed in *nup116* null mutants at 37°C (Wente and Blobel, 1993).

The same strain exhibited a marked difference in morphology when *NUP170* overexpression was induced. Instead of a distorted nuclear envelope, intranuclear annulate lamellae were observed in many instances (Fig. 9). As was the case with the depletion phenotype, these structures are not a direct result of the overexpression of *NUP170*, but their formation requires the overexpression of *NUP170* in the absence of *POM152*. Intranuclear annulate lamellae have also been observed in *nup116* null mutants by Wente and Blobel (1993). However unlike the annulate lamellae observed in the *nup116Δ* strain, we have not observed an attachment between the intranuclear annulate lamellae and the inner nuclear membrane.

The nuclear envelope abnormalities we have observed here by varying the expression levels of *NUP170*, within a *pom152Δ* background, suggests that the maintenance of proper stoichiometry between constituents of the NPC is important. Variations in *NUP170* expression above and below wild-type levels of Nup170p leads to distinct phenotypes. The primary effect of these abnormalities is impossible to determine using the techniques employed here. The effects we observe are likely to be pleiotropic, resulting from a reduced ability for the NPC to perform any number of its many functions, including interactions with the underlying chromatin and/or nuclear matrix, changes in the overall bidirectional transport rate, or an imbalance of transport. The fact that overlapping phenotypes are observed in *nup1* (Bogerd et al., 1994) and *nup116* (Wente and Blobel, 1993) mutants also indicates the effects we observe are many fold. Likewise, very little insight would be expected to be gained from employing an in vivo transport assay on different carbon sources. Any effect observed could equally be attributed to pleiotropic effects and, since the cells are viable under these conditions, bidirectional transport must be taking place. We, in fact, did not detect any mRNA transport defects associated with the depletion or overexpression of *NUP170* in strains lacking *POM152* (data not shown).

Nup170p and Nup157p are abundant evolutionarily conserved nucleoporins, and *nup170* synthetic lethal mutants can be complemented by mammalian *NUP155*. This likely reflects their similar roles as proteins of the core framework of NPCs. Recently, structurally and functionally homologous nuclear transport factors have been found in both vertebrates and yeast. Taken together these observations underscore the fundamental similarities between the structure and function of all eukaryotic NPCs.

We thank The Rockefeller University/Howard Hughes Medical Institute Biopolymer Facility for oligonucleotide synthesis and peptide sequencing, especially Joseph Fernandez; Eleana Sphicas for assistance in performing the electron microscopy studies; Drs. Ulf Nehrbass and Felix Kessler for helpful discussions; Shawna Maguire for helpful discussions and technical assistance; and Ramsey Saleem for technical assistance.

J. D. Aitchison is a Medical Research Council of Canada Postdoctoral Fellow; R. W. Wozniak is an Alberta Heritage Scholar. This work as supported in part by an operating grant from the Medical Research Council of Canada.

Received for publication 10 July 1995 and in revised form 25 August 1995.

References

Adam, E. J., and S. A. Adam. 1994. Identification of cytosolic factors required for nuclear location sequence-mediated binding to the nuclear envelope. *J. Cell Biol.* 125:547–555.

Adam, S. A., R. S. Marr, and L. Gerace. 1990. Nuclear protein import in permeabilized mammalian cells requires soluble cytoplasmic factors. *J. Cell Biol.* 111:807–816.

Aitchison, J. D., W. W. Murray, and R. A. Rachubinski. 1991. The carboxy-terminal tripeptide Ala-Lys-Ile is essential for targeting *Candida tropicalis* trifunctional enzyme to yeast peroxisomes. *J. Biol. Chem.* 266:23197–23303.

Akey, C. W., and M. Radermacher. 1993. Architecture of the Xenopus nuclear pore complex revealed by three dimensional cryo-electron microscopy. *J. Cell Biol.* 122:1–19.

Ammerer, G. 1983. Expression of genes in yeast using the ADC1 promoter. *Methods Enzymol.* 101:192–201.

Ausubel, F. M., R. Brent, R. E. Kingston, D. D. Moore, J. G. Seidman, J. A. Smith, and K. Struhl. 1992. Short Protocols in Molecular Biology. Greene Publishing Associates, New York.

Belanger, K. D., M. A. Kenna, S. Wei, and L. I. Davis. 1994. Genetic and physical interactions between Srp1p and nuclear pore complex proteins Nup1p and Nup2p. *J. Cell Biol.* 126:619–630.

Bender, A., and J. R. Pringle. 1991. Use of a synthetic lethal and multicopy suppressor mutant to identify two new genes involved in morphogenesis in *Saccharomyces cerevisiae*. *Mol. Cell. Biol.* 11:1295–1305.

Blobel, G. 1985. Gene gating: a hypothesis. *Proc. Natl. Acad. Sci. USA.* 82: 8527–8529.

Bogerd, A. M., J. A. Hoffman, D. C. Amberg, G. R. Fink, and L. I. Davis. 1994. *nup1* mutants exhibit pleiotropic defects in nuclear pore complex function. *J. Cell Biol.* 127:319–332.

Burnette, W. N. 1981. "Western blotting": electrophoretic transfer of proteins from sodium dodecyl sulfate-polyacrylamide gels to unmodified nitrocellulose and radiographic detection with antibody and radioiodinated protein A. *Anal. Biochem.* 112:195–203.

Byers, B., and L. Goetsch. 1991. Preparation of yeast cell for thin-section electron microscopy. *Methods Enzymol.* 194:602–608.

Byrd, D. A., D. J. Sweet, N. Pante, K. N. Konstantinov, T. Guan, A. C. S. Saphire, P. J. Mitchell, C. S. Cooper, U. Aebi, and L. Gerace. 1994. Tpr, a large coiled coil protein whose amino terminus is involved in activation of oncogenic kinases, is localized to the cytoplasmic surface of the nuclear pore complex. *J. Cell Biol.* 127:1515–1526.

Cesareni, G., and J. A. H. Murray. 1987. Plasmid vectors carrying the replication origin of filamentous single-stranded phages. *Genet. Eng.* 9:135–154.

Christianson, T. W., R. S. Sikorski, M. Dante, J. H. Shero, and P. Hieter. 1992. Multifunctional yeast high-copy-number shuttle vectors. *Gene.* 110:119–122.

Delorme, E. 1989. Transformation of *Saccharomyces cerevisiae* by electroporation. *Appl. Environ. Microbiol.* 55:2242–2246.

Enenkel, C., G. Blobel, and M. Rexach. 1995. A yeast karyopherin heterodimer that targets proteins to nuclear pores. *J. Biol. Chem.* 270:16499–16502.

Fernandez, J., L. Andrews, and S. M. Mische. 1994. An improved procedure for enzymatic digestion of polyvinyldiene difluoride-bound proteins for internal sequence analysis. *Anal. Biochem.* 218:112–117.

Forbes, D. J. 1992. Structure and function of the nuclear pore complex. *Annu. Rev. Cell Biol.* 8:495–527.

Goldberg, M. W., J. J. Blow, and T. D. Allen. 1992. The use of field emission inlens scanning electron microscopy to study the steps of assembly of the nuclear envelope in vitro. *J. Struct. Biol.* 108:257–268.

Görlich, D., S. Prehn, R. A. Laskey, and E. Hartmann. 1994. Isolation of a protein that is essential for the first step of nuclear protein import. *Cell.* 79:767–778.

Görlich, D., S. Kostka, R. Kraft, C. Dingwall, R. A. Laskey, E. Hartmann, and S. Prehn. 1995. Two different subunits of importin cooperate to recognize nuclear localization signals and bind them to the nuclear envelope. *Curr. Biol.* 5:383–392.

Gorsch, L. C., T. C. Dockendorff, and C. N. Cole. 1995. A conditional allele of the novel repeat-containing yeast nucleoporin RAT7/NUP159 causes both rapid cessation of mRNA export and reversible clustering of nuclear pore complexes. *J. Cell Biol.* 129:939–955.

Grandi, P., V. Doye, and E. C. Hurt. 1993. Purification of NSP1 reveals complex formation with 'GLFG' nucleoporins and a novel nuclear pore protein NIC96. *EMBO J.* 12:3061–3071.

Grandi, P., N. Schlaich, H. Tekotte, and E. C. Hurt. 1995. Functional interaction of Nic96p with a core nucleoporin complex consisting of Nsp1p, Nup49p and a novel protein Nup57p. *EMBO J.* 14:76–87.

Hallberg, E., R. W. Wozniak, and G. Blobel. 1993. An integral membrane protein of the pore membrane domain of the nuclear envelope contains a nucleoporin-like region. *J. Cell Biol.* 122:513–521.

Higgans, D. G., and P. M. Sharp. 1989. Fast and sensitive multiple sequence alignments on a microcomputer. *CABIOS*. 5:151–153.

Hinshaw, J. E., B. O. Carragher, and R. A. Milligan. 1992. Architecture and design of the nuclear pore complex. *Cell*. 69:1133–1141.

Jarnik, M., and U. Aebi. 1991. Toward a more complete 3-D structure of the nuclear pore complex. *J. Struct. Biol.* 107:291–308.

Jones, J. S., and L. Prakash. 1990. Yeast *Saccharomyces cerevisiae* selectable markers in pUC18 polylinker. *Yeast*. 6:363–366.

Kilmartin, J. V., and A. E. Adams. 1984. Structural rearrangements of tubulin and actin during the cell cycle of the yeast *Saccharomyces*. *J. Cell Biol.* 98: 922–933.

Koshland, D., J. C. Kent, and L. H. Hartwell. 1985. Genetic analysis of the mitotic transmission of mini chromosomes. *Cell*. 40:493–503.

Kraemer, D., R. W. Wozniak, G. Blobel, and A. Radu. 1994. The human CAN protein, a putative oncogene product associated with myeloid leukemogenesis, is a nuclear pore complex protein that faces the cytoplasm. *Proc. Natl. Acad. Sci. USA*. 91:1519–1523.

Kraemer, D. M., C. Strambio-de-Castillia, G. Blobel, and M. P. Rout. 1995. The essential yeast nucleoporin NUP159 is located on the cytoplasmic side of the nucelar pore complex and serves in karyopherin-mediated binding of transport substrate. *J. Biol. Chem.* 270:19017–19021.

Kranz, J. E., and C. Holm. 1990. Cloning by function: an alternative approach for identifying yeast homologs of genes from other organisms. *Proc. Natl. Acad. Sci. USA*. 87:6629–6633.

Kyte, J., and R. F. Doolittle. 1982. A simple method for displaying the hydropathic character of a protein. *J. Mol. Biol.* 157:105–132.

Maul, G. G. 1977. The nuclear and the cytoplasmic pore complex: structure, dynamics, distribution, and evolution. *Int. Rev. Cytol. Suppl.* 5:75–186.

Moore, M. S., and G. Blobel. 1992. The two steps of nuclear import, targeting to the nuclear envelope and translocation through the nuclear pore, require different cytosolic factors. *Cell*. 69:939–950.

Moore, M. S., and G. Blobel. 1993. The GTP-binding protein Ran/TC4 is required for protein import into the nucleus. *Nature (Lond.)*. 365:661–663.

Moroianu, J., G. Blobel, and A. Radu. 1995. A previously identified protein of uncertain function is karyopherin-α and together with karyopherin-β docks import substrate at nuclear pore complexes. *Proc. Natl. Acad. Sci. USA*. 92: 2088–2091.

Newmeyer, D. D., and D. J. Forbes. 1990. An N-ethylmaleimide-sensitive cytosolic factor necessary for nuclear protein import: requirement in signal-mediated binding to the nuclear pore. *J. Cell Biol.* 110:547–557.

Pearson, W. R., and D. J. Lipman. 1988. Improved tools for biological sequence comparison. *Proc. Natl. Acad. Sci. USA*. 85:2444–2448.

Radu, A., G. Blobel, and R. W. Wozniak. 1993. Nup155 is a novel nuclear pore complex protein that contains neither repetitive sequence motifs nor reacts with WGA. *J. Cell Biol.* 121:1–9.

Radu, A., G. Blobel, and M. S. Moore. 1995*a*. Identification of a protein complex that is required for nuclear import and mediates docking of import substrate to distinct nucleoporins. *Proc. Natl. Acad. Sci. USA*. 92:1769–1773.

Radu, A., M. S. Moore, and G. Blobel. 1995*b*. The peptide repeat domain of nucleoporin Nup98 functions as a docking site in transport across the nuclear pore complex. *Cell*. 81:215–222.

Ris, H., and M. Malecki. 1993. High-resolution field emission scanning electron microscope imaging of internal cell structures after Epon extraction from sections: a new approach to correlative ultrastructural and immunocytochemical studies. *J. Struct. Biol.* 111:148–157.

Rose, M., P. Grisafi, and D. Botstein. 1984. Structure and function of the yeast *URA3* gene: expression in *Escherichia coli*. *Gene*. 29:113–124.

Rothstein, R. 1991. Targeting, disruption, replacement, and allele rescue: integrative DNA transformation in yeast. Methods Enzymol. 194:281–301.

Rout, M. P., and G. Blobel. 1993. Isolation of the yeast nuclear pore complex. *J. Cell Biol.* 123:771–783.

Rout, M. P., and S. R. Wente. 1994. Pores for thought: nuclear pore complex proteins. *Trends Cell Biol.* 4:357–365.

Sherman, F., G. R. Fink, and J. B. Hicks. 1986. Methods in Yeast Genetics. Cold Spring Harbor Laboratory Press, Cold Spring Harbor, New York. 186 pp.

Sikorski, R. S., and P. Hieter. 1989. A system of shuttle vectors and yeast host strains designed for efficient manipulation of DNA in Saccharomyces cerevisiae. *Genetics*. 122:19–27.

Strathern, J. N., and D. R. Higgins. 1991. Recovery of plasmids from yeast into *Escherichia coli*: shuttle vectors. *Methods Enzymol.* 194:319–329.

Sukegawa, J., and G. Blobel. 1993. A nuclear pore complex protein that contains zinc finger motifs, binds DNA, and faces the nucleoplasm. *Cell*. 72:29–38.

Uhlen, M., B. Guss, B. Nilsson, S. Gatenback, L. Philipson, and M. Lindberg. 1984. Complete sequence of the staphylococcal gene encoding protein A: a gene evolved through multiple duplications. *J. Biol. Chem.* 259:13628–13638.

Unwin, P. N., and R. A. Milligan. 1982. A large particle associated with the perimeter of the nuclear pore complex. *J. Cell Biol.* 93:63–75.

Weis, K., I. W. Mattaj, A. I. Camond. 1995. Identification of hSRP1a as a functional receptor for nuclear localization signals. *Science (Wash. DC)*. 268: 1049–1053.

Wente, S. R., and G. Blobel. 1993. A temperature-sensitive NUP116 null mutant forms a nuclear envelope seal over the yeast nuclear pore complex thereby blocking nucleocytoplasmic traffic. *J. Cell Biol.* 123:275–284.

Wente, S. R., and G. Blobel. 1994. NUP145 encodes a novel yeast glycine-leucine-phenylalanine-glycine (GLFG) nucleoporin required for nuclear envelope structure. *J. Cell Biol.* 125:955–969.

Wente, S. R., M. P. Rout, and G. Blobel. 1992. A new family of yeast nuclear pore complex proteins. *J. Cell Biol.* 119:705–723.

Wimmer, C., V. Doye, P. Grandi, U. Nehrbass, and E. C. Hurt. 1992. A new subclass of nucleoporins that functionally interact with nuclear pore protein NSP1. *EMBO J.* 11:5051–5061.

Wozniak, R. W., G. Blobel, and M. P. Rout. 1994. POM152 is an integral protein of the pore membrane domain of the yeast nuclear envelope. *J. Cell Biol.* 125:31–42.

Wu, J., M. J. Matunis, D. Kraemer, G. Blobel, and E. Coutavas. 1995. Nup358, a cytoplasmically exposed nucleoporin with peptide repeats, ranGTP binding sites, zinc fingers, a cyclophillinA homologous domain and a leucine rich region. *J. Biol. Chem.* 270:14209–14213.